CLEARINGHOUSE FOR FEDERAL SCIENTIFIC AND TECHNICAL INFORMATION CFSTI
DOCUMENT MANAGEMENT BRANCH 410.11

LIMITATIONS IN REPRODUCTION QUALITY

ACCESSION # AD 605729

☒ 1. WE REGRET THAT LEGIBILITY OF THIS DOCUMENT IS IN PART UNSATISFACTORY. REPRODUCTION HAS BEEN MADE FROM BEST AVAILABLE COPY.

☒ 2. A PORTION OF THE ORIGINAL DOCUMENT CONTAINS FINE DETAIL WHICH MAY MAKE READING OF PHOTOCOPY DIFFICULT.

☐ 3. THE ORIGINAL DOCUMENT CONTAINS COLOR, BUT DISTRIBUTION COPIES ARE AVAILABLE IN BLACK-AND-WHITE REPRODUCTION ONLY.

☐ 4. THE INITIAL DISTRIBUTION COPIES CONTAIN COLOR WHICH WILL BE SHOWN IN BLACK-AND-WHITE WHEN IT IS NECESSARY TO REPRINT.

☐ 5. LIMITED SUPPLY ON HAND: WHEN EXHAUSTED, DOCUMENT WILL BE AVAILABLE IN MICROFICHE ONLY.

☐ 6. LIMITED SUPPLY ON HAND: WHEN EXHAUSTED DOCUMENT WILL NOT BE AVAILABLE.

☐ 7. DOCUMENT IS AVAILABLE IN MICROFICHE ONLY.

☐ 8. DOCUMENT AVAILABLE ON LOAN FROM CFSTI (TT DOCUMENTS ONLY).

☐ 9.

NBS 9/64

PROCESSOR: [signature]

University of Utah

Department of Chemical Engineering

Salt Lake City, Utah

This research was supported by the Propulsion Division, AFOSR, SREP under Contract/Grant AF 49(638)-62

AF AFOSR 40-63

UNIVERSITY OF UTAH DEPARTMENT OF CHEMICAL ENGINEERING

AF AFOSR 40-63

Technical Report

on

IGNITION AND COMBUSTION OF SOLID PROPELLANTS

~~Under Air Force Grant 40-63~~

October 1, 1962 to September 30, 1963

Report prepared by:

Rex C. Mitchell
John A. Keller
Alva D. Baer, Investigator
Norman W. Ryan, Principal Investigator

Report approved by:

Norman W. Ryan

Norman W. Ryan

TABLE OF CONTENTS

or

SUMMARY

This report summarizes work performed under Air Force Grant AFOSR 40-63. The spreading rate of the flame zone on the surface of a solid propellant was studied by use of a rarefaction tube. Cold gas flow past the burning zone and across the unburned surface produced high flame spread velocities. The experimental data were interpreted and correlated in terms of two theoretically predicted but experimentally determined parameters. One parameter which is related to the maximum heat flux produced near the flame front was found to be independent of gas velocity. The second parameter which determines the rate of decay of heat flux ahead of the flame front was found to be independent of pressure.

Data obtained by subjecting composite propellant surfaces to thermal radiation fluxes in the range of 2-13 cal/(sec)(sq cm) were adequately explained in terms of a simple ignition theory. A comparison of the ignition characteristics of several types of catalyzed, composite ammonium-based propellants and of propellant type materials formed by pressing AP and non-volatile carbon black or graphite indicated that, in the range of heat fluxes studied, ignition occurs by decomposition of AP followed by a reaction between the decomposition products and solid fuel binder. A proposed ignition system in which a diffusion flame of propane and oxygen is the energy source was studied in small scale tests. Heat fluxes high enough to produce rapid propellant ignition were obtained.

I. INTRODUCTION

As part of a continuing research effort, several phases of the ignition of composite propellants have been studied. This work was supported by the Air Force Office of Scientific Research under Air Force Grant AF-AFOSR 40-63 and is being continued under Air Force Grant AF-AFOSR 40-64.

In several areas of study, notably on the flame spread across the burning propellant surface and on the ignition response of composite propellants subjected to low radiant heat fluxes (2-13 cal/(sec)(sq cm), the results presented represent essential completion of the proposed work. In the case of the studies of the propellant fuel binder reactions and of the proposed ignition by radiation from a gaseous diffusion flame, only preliminary results are presented. Although much has been done on propellant ignition by high convective heat fluxes (20-100 cal/(sec)(sq cm)) and on the formulation of an ignition theory, the results of these efforts are not in final form. Each of the above studies is discussed in the following sections of this report.

II. FLAME SPREAD ON SOLID PROPELLANT

When a large solid propellant engine is ignited, it is usually the case that only a part of the exposed surface area of the grain is ignited directly by igniter action. The grain surface initially ignited then provides the energy needed to ignite the remaining surface. Very little work has been reported on flame spread assisted by gas flow, even though the process is an important step in the over-all ignition process.

This section presents the results of a study of flow-assisted flame spread over the freshly cut surface of a composite propellant. Experimental conditions of constant pressure and velocity were maintained in each run, and the progress of the flame across the surface was observed by means of high speed photography. The flame spread observations are interpreted in terms of a theoretical description whose success is assured in part by the use of experimental observations to select the form of a key relationship, but validated further by auxiliary studies and by a check with independent ignition measurements.

Theory

The theory developed below pictures the flow of hot combustion products across a flat, unignited surface. The pressure and the free stream velocity are constant. With reference to Figure 1, we take the position of interest to be a distance x from the initial edge of the burning zone; the propellant at position x begins to burn at time t_i. We define an intermediate condition: at time s, the burning zone has approached to a distance y from the position of interest. At time zero, the propellant is at uniform temperature, gas flow is started, and all parts of the surface are instantaneously subjected to heat flow from the hot gases swept past. The time required to establish the quasi-steady-state flow regime is less than 0.1 msec., a negligible interval compared to the times measured.

The following assumptions are made: (1) heat flow to and in the propellant slab is one-dimensional, perpendicular to the surface; (2) the propellant slab is a chemically passive, semi-infinite body of constant thermal properties (density, thermal conductivity, heat capacity) at temperatures below T_i; (3) ignition takes place when the surface temperature reaches a value T_i (computed in accordance with Assumption (2)) characteristic of the propellant; (4) given pressure and free stream velocity, the heat flux is a function only of the distance of the point of interest from the flame front.

The first assumption can be justified by a comparison of temperature gradients, normal and parallel, at the surface. It is sufficient, however, to justify it indirectly by comparing flame spread rates without gas flow (heat transfer along the surface) to rates with gas flow (added flux, normal, from the gas phase). Without, the rate is less than twice the normal burning rate [8]; with, the rate is from 40 to 400 times the normal burning rate under the conditions of this study. The second assumption is a convenience, and derives its justification from the success of the third assumption. The third assumption is known to be a good approximation for the pressures and convective flux levels of this study [2, 3, 6]. The fourth assumption depends for its justification on the ability of the analysis which follows to correlate the experimental results.

The one-dimensional, unsteady-state heat transfer equation for a semi-infinite solid extending from $z = 0$ to $z = \infty$,

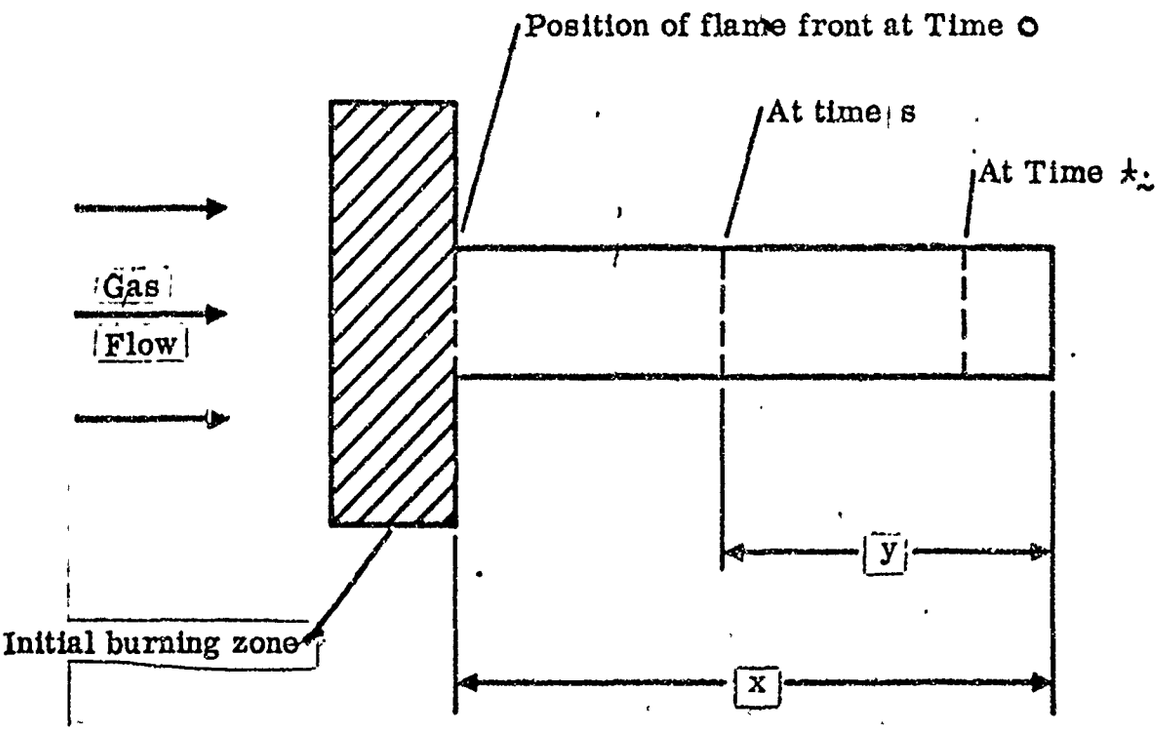

Fig. 1. Diagram of Propellant Slab

$$\frac{\partial T}{\partial z} = \frac{k}{\rho c} \frac{\partial^2 T}{\partial z^2} \tag{1}$$

can be solved with the boundary conditions

$$f = -k \frac{\partial T}{\partial z} \quad \text{at } z = 0, \ \theta > 0$$

$$T(z) = 0 \text{ at } \theta \leqslant 0$$

$$T(\theta) = 0 \text{ in limit } z \longrightarrow \infty$$

to give the following result for the surface temperature rise [4].

$$T(\theta)_{z=0} = \frac{1}{\Gamma\sqrt{\pi}} \int_0^{\theta} \frac{f_i(s)}{\sqrt{\theta - s}} \, ds \tag{2}$$

For the present model, Equation (2) can be written as

$$T_i = \frac{1}{\Gamma\sqrt{\pi}} \int_0^{t_i} \frac{f_2(s,x)}{\sqrt{t - s}} \, ds \tag{3}$$

where it is noted that the surface heat flux is a function of both elapsed time and the position of interest. As T_i is a constant, Equation (3) is an implicit relationship between x and t_i. According to Assumption (4), $f_2(s,x)$ can be expressed as f(y). As the heat flux is expected to approach zero for large values of y and to be a maximum value, f_o, adjacent to the flame front where y = 0, it seems reasonable to invoke Assumption (4) as

$$f = f_2(s,x) = f_o \, \psi(\alpha y) \tag{4}$$

where α is a parameter having dimensions of reciprocal length whose purpose is to form the dimensionless distance variables αy and αx.

Equation (3) is now written

$$T_i = \frac{f_o}{\Gamma\sqrt{\pi}} \int_0^{t_i} \frac{\psi(\alpha y)}{\sqrt{t - s}} \, ds \tag{5}$$

If we assign a suitable specific form to $\psi(\alpha y)$ and utilize the fact that $(x - y)$ is the same function of s as x is of t_i, we can in principle extract a unique x(t) relationship from Equation (5). In dimensionless form that is not committed to values of T_i, f_o, Γ, but is committed to the form of $\psi(\alpha y)$, we can get

$$\alpha x = \Phi(\tau) \tag{6}$$

where dimensionless time (τ) and the time parameter (β) are defined as

$$\tau_i = \beta\, t_i = \left(\frac{4\, f_o^{\,2}}{\pi \Gamma^2 T_i^{\,2}} \right) t_i \qquad (7)$$

The chore remaining is to find $\psi(\alpha y)$; then to express Equation (6) in useful form.

A very approximate analysis of heat transfer from gas to solid through a laminar boundary layer [7] suggests that reasonable forms of $\psi(\alpha y)$ might be

$$\psi(\alpha y) = e^{-\alpha y} \quad \text{or} \quad \psi(\alpha y) = (1 + \alpha y)^{-n}$$

Both of these forms, the latter with n of 1/5, 1/2, and 2, were employed with Equation (5) (altered for computational convenience) to produce the relationship (6) via a tedious numerical procedure. Table I gives the relationship for

$$(\alpha y) = (1 + \alpha y)^{-1/2} \qquad (8)$$

which, on grounds to be discussed later, was selected as most satisfactory.

Equation (5) can be written

$$\tau^{-1/2} = \frac{T_i \Gamma \sqrt{\pi}}{2\, f_o \sqrt{t}} = \frac{1}{2} \int_0^1 \frac{\psi(\alpha y)}{\sqrt{1 - \frac{s}{t}}}\, d\left(\frac{s}{t_i} \right) \qquad (9)$$

If, at time θ the temperature at x is T, we can also write

$$\frac{T \Gamma \sqrt{\pi}}{2\, f_o \sqrt{\theta}} = \frac{1}{2} \int_0^{\theta/t_i} \frac{\psi(\alpha y)}{\sqrt{1 - \frac{s}{t}}}\, d\left(\frac{s}{t_i} \right) \qquad (10)$$

Equation (10) divided by Equation (9) gives T/T_i as a function of $\theta\, \tau_i/t_i$, with αx as parameter. This relationship is shown as the curves on Figure 3 for three values of αx. Again Equation (3) was used.

One additional observation is to be made. If we take $\alpha x = 0$, that is, we direct attention to the part of the surface adjacent to the initial flame front at $s = 0+$, we find (neglecting the slow, unassisted flame spread) that a finite time, t_o, is needed to start the flame spread. All suitable forms

of $\psi(\alpha y)$ must give $\psi(0) = 1$. Equation (9) yields $\tau_i = 1$ for $x = 0$, or, from Equation (7),

$$t_i f_o^2 = \frac{\pi}{4} r^2 T_i^2 \qquad (11)$$

Equation (11) is one of the basic relationships employed by Baer [2, 3] and McCune [6] to interpret convective flux ignition data. It thus provides a bridge between this study and other information about the ignition of Utah F propellant.

Experiment

The rarefaction tube was found to be a convenient tool for producing controlled conditions of constant pressure and gas velocity As used in this study, the rarefaction tube was a tube of circular cross-section, closed at one end and fitted with a nozzle at the other. The tube was initially pressurized with a diaphragm over the nozzle, then the diaphragm was broken to produce a rarefaction or expansion wave. Test pressure and gas velocity are determined by the initial pressure and the ratio of nozzle area to tube area. This use of the rarefaction tube is discussed in a previous report [8].

The tubes employed in this study were of 1-7/8 inch inside diameter and lengths up to sixty-five feet, permitting test times up to 110 milliseconds. The test section, see Figure 2, was a short section of clear lucite tubing with a glass insert 1-7/8 inch in inside diameter to protect the lucite from the flame. The T-shaped propellant samples were mounted in a slot milled in the top surface of a streamlined brass plate. This was bolted to a non-conducting pedestal which also served as a mounting block for electrical and instrument connections. The actual flame spread was observed by means of high-speed motion pictures taken with a Wollensak "Fastax" camera at speeds of 1000 to 2000 frames per second.

The propellant, designated as Utah F, used in this study was a composite, non-aluminized propellant containing 80 weight per cent ammonium perchlorate, 18 per cent butadiene-acrylic acid copolymer binder, and 2 per cent copper chromite burning rate catalyst. The strand burning rate can be approximately described by the equation

$$r(\text{cm/sec}) = 0\ 312\ p^{0.40} \quad (\text{with p in atm.})$$

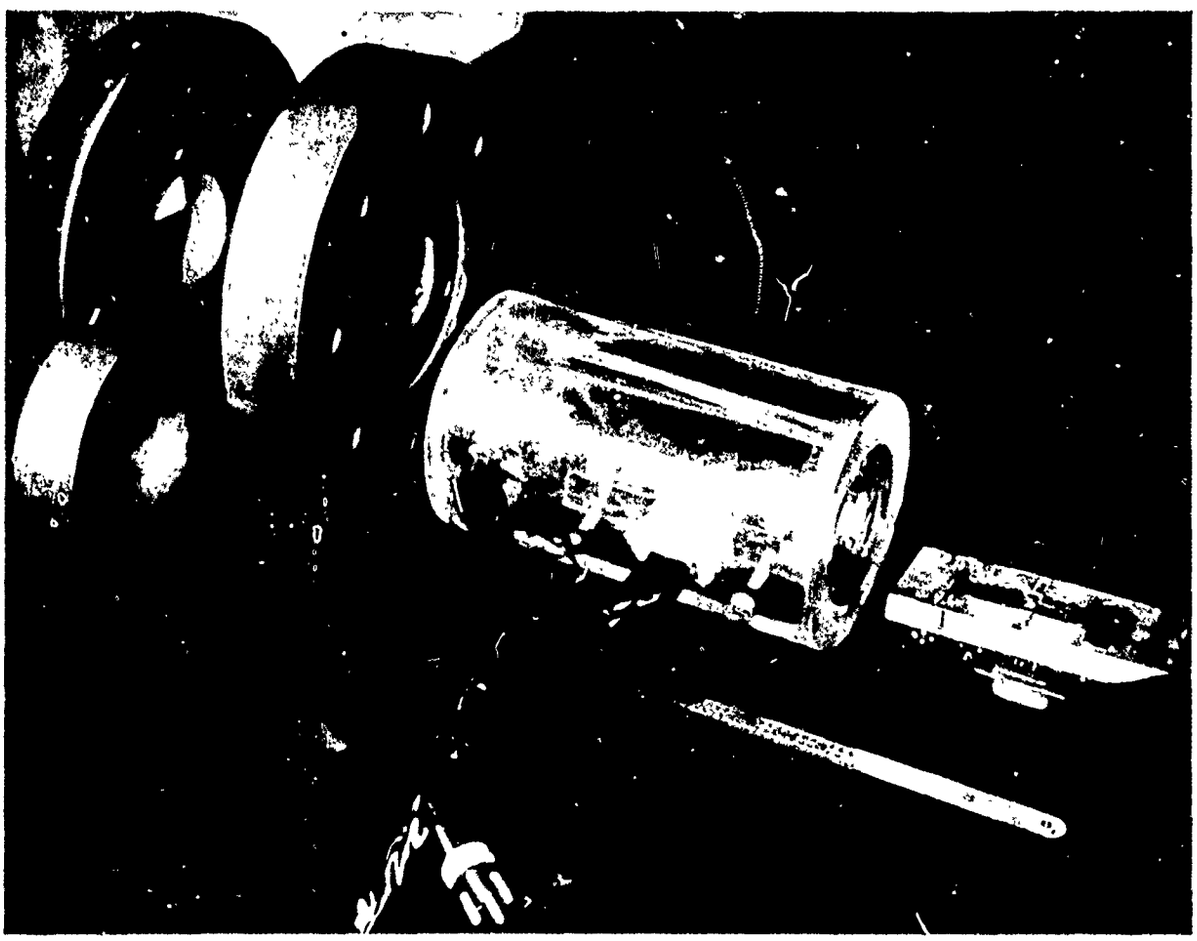

Figure 2. Exploded view, from left to right, of end flange, nozzle, intermediate flange, test section, and sample holder with temperature gauge in place.

In an experimental flame spread run the T-shaped propellant slab was initially ignited across the upstream width with a hot wire After a specified time interval, long enough to allow the propellant to reach steady burning, but short enough to minimize preheating of the unignited part of the slab, the diaphragm over the nozzle of the rarefaction tube was broken to start the rarefaction. The pressure-time oscilloscope traces and high-speed motion pictures of the burning slab were used to obtain the gas conditions during the test period and the distance of flame spread as a function of time, respectively.

An auxiliary study to measure temperature as a function of time at the propellant surface was made. These measurements were made with thin-film platinum resistance thermometers bonded to fired prophylite bases. These sensors were mounted just downstream from the propellant slab. The details of the experimental work are discussed by Mitchell [7]. The temperature-time oscilloscope traces obtained were compared with the theoretical temperature-time curves calculated from Equations (9) and (10).

Discussion

The choice of $\psi(\alpha y)$, Equation (8), was based on experimental results as follows. The αx, τ relationship, of which Table I is one example, for each of the candidate $\psi(\alpha y)$ functions was plotted on logarithmic coordinates. Experimental x,t data were plotted on another graph, also on logarithmic coordinates and to the same scale. Superposition of the graphs allowed qualitative comparison of the experimental and the theoretical curves, and led to the selection of Equation (8) as the form of $\psi(\alpha y)$ conforming best to experiment. The curve matching was used also for quantitative purposes. When the curves are matched, any pair of matched coordinates $(\tau,\alpha x)$ and (t,x) can be used to compute α and β from

$$\alpha = \frac{(\alpha x)}{x} \qquad \text{and} \qquad \beta = \frac{\tau}{t}$$

This procedure was employed.

The selection of $\psi(\alpha y)$ as described above was further confirmed by a plot of experimental temperature-time data on Figure 3, where agreement is considered satisfactory. The preparation of the data for plotting on Figure 3 required correcting gage temperature for the difference in properties between propellant and fired pyrophylite [5]. If we assume the heat flux is the same to both propellant and the gage,

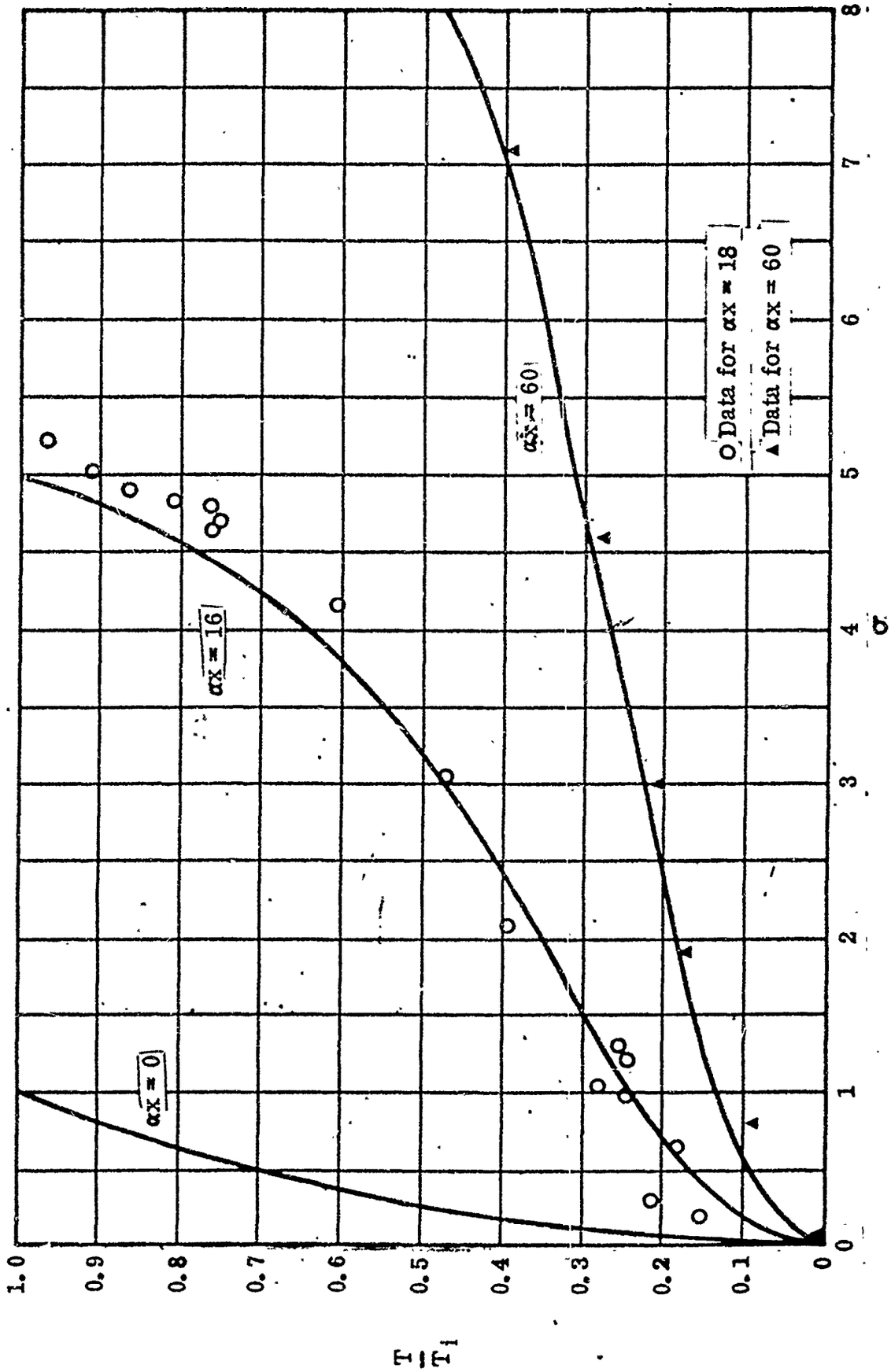

Fig. 3. Theoretical temperature-time curves, in dimensionless form, with examples of experimental data.

$$T_i \text{ (gage)} = \frac{\Gamma \text{(propellant)}}{\Gamma \text{(gage)}} \; T_i \text{ (propellant)}$$

in accordance with Equation (9). The value of T_i for the propellant and the value of f_o are obtained by the simultaneous solution of Equation (7) with the known β and an approximate relationship derived from the data of Keller [5] who studied high convective flux ignition of Utah F propellant.

$$T_i \text{ (deg. C.)} = 250 + 1.53 \; f_o \text{ (cal/sq.cm./sec)}. \qquad (12)$$

$$50 < f_o < 100$$

Keller's data are for constant flux, a condition that does not apply in the study reported here. Nevertheless, the above equation was used, it being assumed that T_i is a function of the propellant and the maximum flux (f_o). Its variation from test to test is absorbed in the pressure and velocity dependence of β. This relaxation of Assumption (3) does not invalidate the developments in the section on Theory.

The rates of flame spread observed in this study, expressed as dx/dt, ranged from 13. centimers per second at the beginning of flame spread for the lowest pressure and velocity, to about 400. centimeters per second after the flame had spread five centimeters and for higher pressures and velocities These extremes represent rates about 40 to 400 times the normal burning rates at the same pressures.

A few observations on the method of flame propagation might be of value. The burning zone seemed to advance by the addition of discrete groups of tiny flames, rather than by the steady onrush of a moving flame front. There appeared, typically, tiny "secondary ignition spots" somewhat in advance of the main flame front. These would begin to spread, but at a slower rate than the advance of the main flame front, so that they were usually overtaken by and consolidated with the main burning area before spreading to an appreciable extent. Although the flame seemed to spread in a series of small, but discrete, jumps, the position-time points indicated reasonably smooth curves when plotted. The secondary ignition spots seemed t occur largely at random, in terms of time, position, and frequency.

- Values of α and β were obtained for the data by the curve-matching technique. These results, along with the gas pressures and velocities, are presented graphically in Figures 4 and 5.

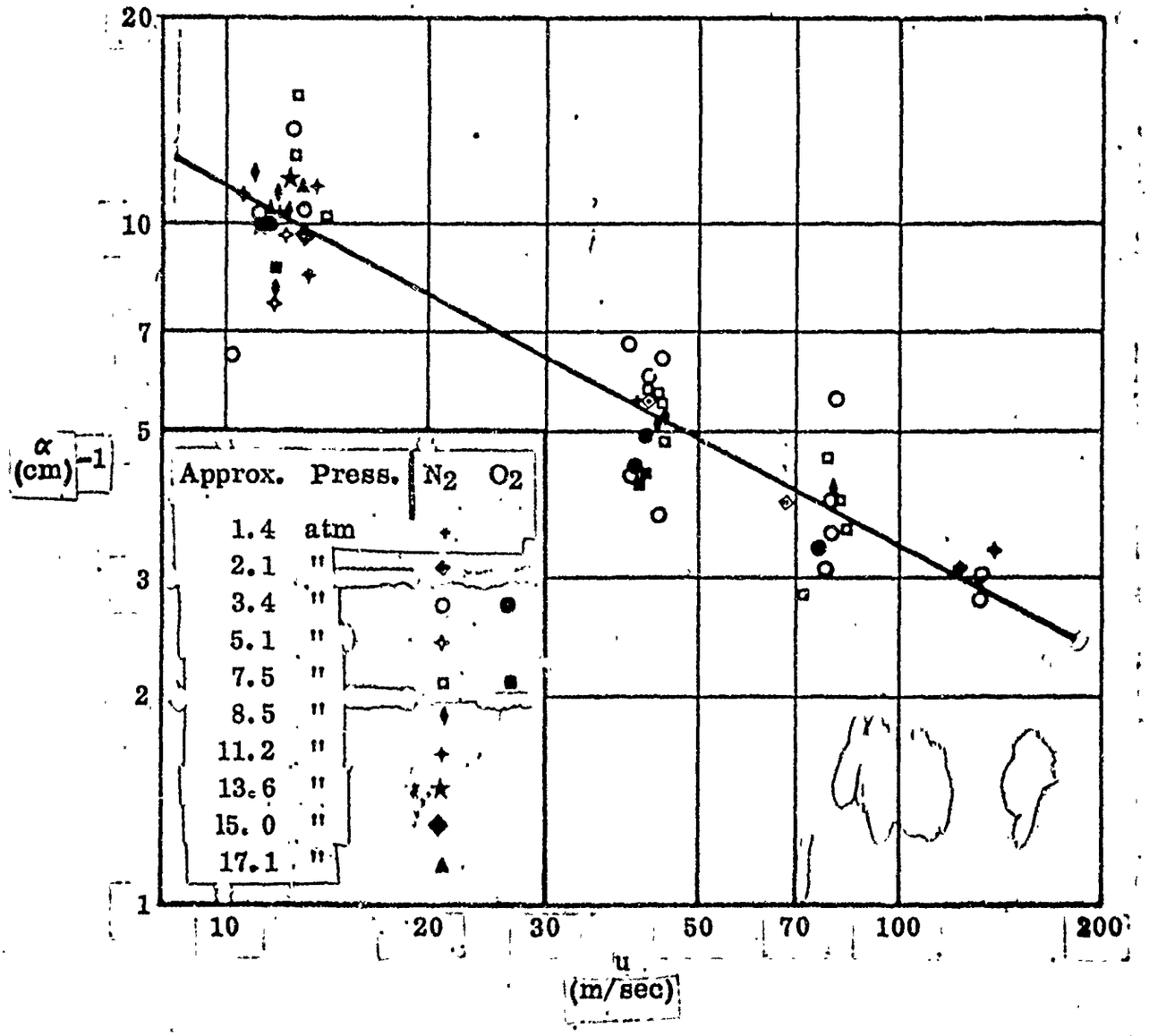

Fig. 4. Correlation of reciprocal distance parameter, α_5 with gas velocity.

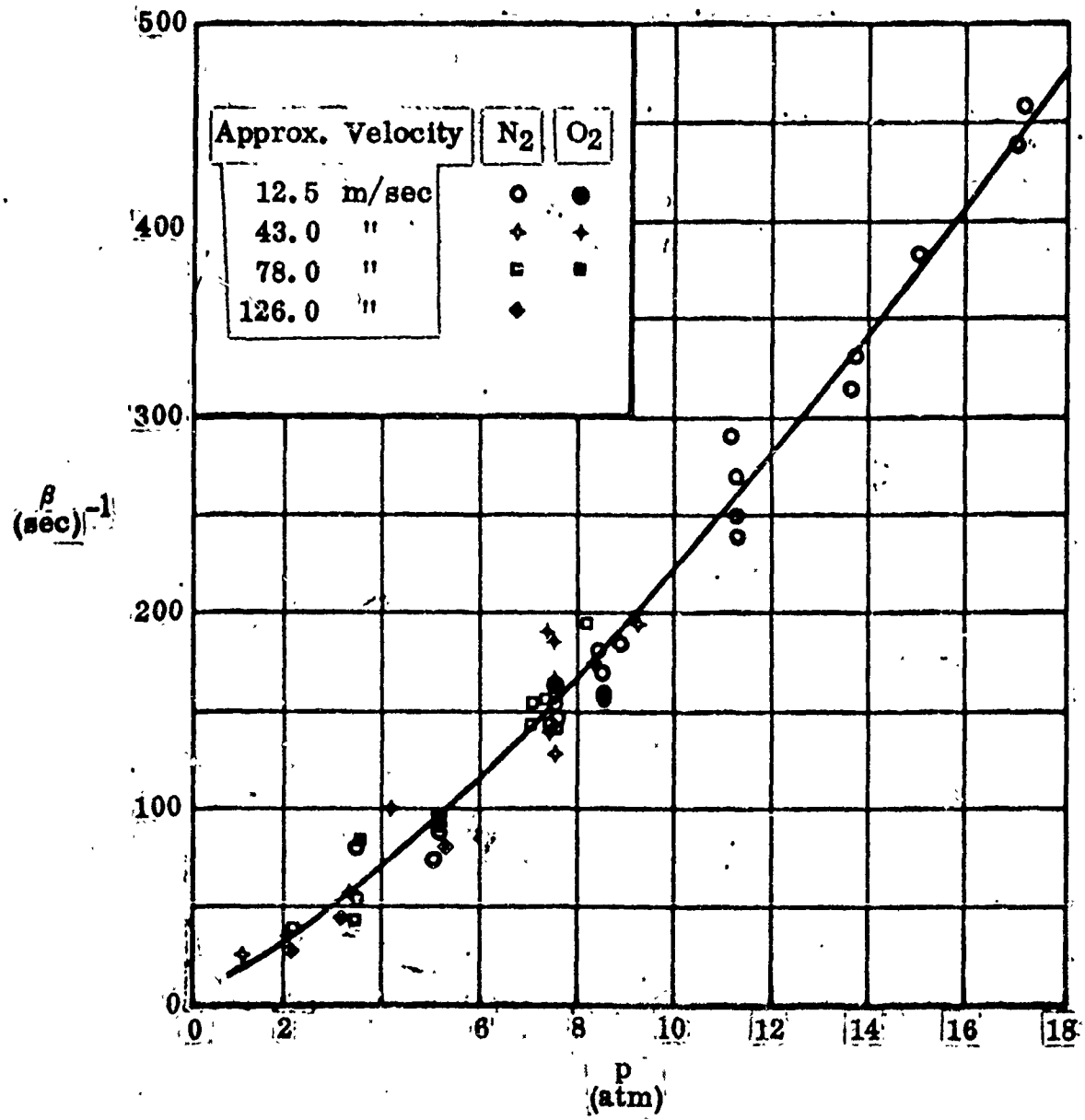

Fig. 5 — Correlation of reciprocal time parameter, β, with pressu

The distance parameter, α, is a strong function of gas velocity but apparently not of pressure, and the time parameter, β, although increasing with increasing pressure, seems to be not affected significantly by velocity. The relationship between α and velocity can be adequately expressed by the equation

$$\alpha u^{.55} = 41.3,$$

where α is expressed in reciprocal centimeters and u in meters per second. The parameter β is approximately proportional to the 1.25 power of pressure.

The nature of the time parameter β is known from the defining Equation (7). The increase in β, that is of f_o^2/T_i, with increasing pressure is explained qualitatively by the increase in density of the hot gas from the burning zone. A greater density of enthalpy is provided at a less rapidly diminishing temperature level as the heat is transferred. If the dependence of T_i on f_o, Equation (12) is taken into account, f_o is found to be nearly proportional to pressure. Apparently the effectiveness of transport of hot gas from the burning zone over contiguous unignited surface is the same at all the velocities studied here (greater than 10 meters per second).

The inverse relationship between α and the velocity is, from boundary layer considerations, to be expected. The empirical origin of α, however, makes it difficult to comment on the degree of velocity dependence and the absence of pressure dependence. Two effects of increasing velocity are easily conceived. First, the boundary layer thickness is reduced and heat transfer thereby enhanced; second, at a given distance from the flame front, the hot gas has had less time to radiate or otherwise lose its energy to the surroundings.

Several runs were made with oxygen as the free stream gas in place of nitrogen. The resulting values of α and β are also plotted on Figures 4 and 5. It is presumed that, if there were a significant degree of mixing of tube gas and combustion products, substitution of oxygen for nitrogen as tube gas would increase the rate of flame spread markedly. Although the tests did give lower values of α and higher values of β than did the similar tests with nitrogen, the differences were small enough to indicate that mixing of ambient gas and combustion products was not extensive. The effect observed could well have been due to burning of the underoxidized combustion products with oxygen at the outer edge of the flame brush. It is concluded that, except to provide the aerodynamic environment, the tube gas did not

sure.

participate significantly.

Equation (11) and the preliminary ignition results of Keller [5], who has ignited Utah F propellant with high convective fluxes, can be used to estimate f_o and T_i values. We are justified only in presenting order of magnitude figures. For β of 60 $sec.^{-1}$, the heat flux is about 50 cal. per (sq. cm., sec.). For β of 450 $sec.^{-1}$, observed for flame spread at 17 atm., some extrapolation gives a flux of about 180 cal per (sq. cm., sec.).

Conclusions

In rocket design practice, we are confronted with the problem of anticipating perhaps of regulating, the progress of ignition over large areas of propellant surface under conditions of changing pressure, energy distribution, and internal flow patterns. Flame spread is the concluding phase of the complex sequence of events that comprise the over-all ignition transient. It is, therefore, the one most susceptible to influence by all the variables of igniter behavior, propellant response, geometry, and scale, insofar as these affect the time-dependent heat flux distribution. From laboratory experiments conducted with constant process conditions, therefore, the principal products expected will be clues to the influence of the process conditions. A by-product is the suggestion that a successful method of analyzing the laboratory data may find application to large-scale problems.

In this study of flow-assisted flame spread, the pressure and the free stream velocity were held constant in each test, varied independently from test to test. The scheme of analysis produces two flame-spread parameters in which, fortuitously, the pressure and velocity effects are isolated. It appears that increasing either pressure or gas velocity accelerates flame spread. For a given fractional change, the influence of pressure is greater than the influence of velocity.

The scheme of analysis is based on two key assumptions that the propellant has a unique ignition temperature, and that, given pressure and velocity, heat flux to the surface depends only on the distance of the point of interest from the flame front. These assumptions may be fruitful in analyzing the more complicated full-scale ignition transient.

III. IGNITION THEORY

As indicated in a previous report [9] the low-flux ignition characteristics of the composite propellants studied can be adequately described by a simple mathematical model. The propellant slab is considered to be a homogeneous, semi-infinite body originally at a uniform temperature and subjected to a constant surface heat flux. These conditions were closely approximated by the experimental conditions. Ignition is assumed to be the result of a runaway exothermic surface reaction which contributes to the surface heat flux. The mathematical relationship which describes this model is that

$$\frac{\partial T}{\partial t} = \frac{\rho c}{k} \frac{\partial^2 T}{\partial z^2} \tag{12}$$

with the boundary condition at $x = 0$

$$-k \frac{\partial T}{\partial z} = f + Be^{-E_b/RT}$$

and as $z \longrightarrow \infty$

$$T = T_o$$

and with the initial condition that $t = 0$

$$T(z) = T_o$$

where T is local absolute temperature, z is the positive distance from the surface into the solid, t is time, F the externally applied heat flux, B the product of the surface reaction frequency factor and the quantity of energy transmitted to the surface per unit reaction, E the effective reaction activation energy, and k, ρ, and c respectively the solid thermal conductivity, density, and heat capacity. T_o is the initial uniform solid temperature. For the purposes of this report, the thermal properties were assumed to be constant at their 60° C. value. In most cases, comparative results only are considered; and, since the major constituent of all materials was the same (AP), the effect of temperature dependence of the thermal properties should be the same for all materials. Equation (12) was put into dimensionless form and numerical solutions were obtained for various reasonable values of the parameters. Ignition was assumed to occur when the surface reaction term was greater than f and was changing rapidly with time.

It appears likely that the actual ignition process is considerably more complex than is indicated by Equation (12); however, this model seems to be an adequate approximation to the controlling processes for the case of low surface flux ignition. A reasonable mechanism which could lead to Equation (13) would be a surface or bulk endothermic reaction followed by a rapid exothermic surface reaction.

An analysis of the results of the numerical solutions of Equation (12) indicates the following characteristics for the propellant ignition:

1. The square root of the calculated ignition times, $\sqrt{t_i}$, are roughly inversely proportional to the surface heat flux. A plot of $\log\sqrt{t_i}$ versus log f should be essentially a straight line of slope slightly greater than minus one The slope of such a plot depends, to a very good approximation, only on the activation energy assumed for the reaction. From the numerical calculations, it is found that

$$S = 4.2\,\frac{RT_o}{E} - 1 \qquad (13)$$

where S is the slope of such a plot. Equation (13) can be used to obtain activation energies from experimental data. Since S is normally close to minus one, small errors in the determination of S can result in large errors in the calculation for E/R.

2. The effect of pressure on the ignition process is determined by the effect of pressure on the parameter B in the boundary condition equation. If the final exothermic reaction in a chain proceeds as rapidly as reactants are formed, the parameter B and the ignition time would be independent of pressure. If B is proportional to pressure, as would be the case if excess reactants were present, numerical solutions indicated that for the range of activation energies anticipated

$$t_i \propto p^n$$

where n ranges from 0.15 to 0.25. In either case, the ignition process would not be a very strong function of pressure.

3. A convenient parameter for use in characterizing solid propellant ignition is the linearly calculated surface temperature at ignition,

T_i. For the case of constant surface heat flux

$$T_i = T_o + \frac{2f}{\Gamma}\sqrt{\frac{t_i}{\pi}} \tag{14}$$

where Γ is the thermal responsivity of the propellant, $\sqrt{k\rho c}$. Equation (14) is just the solution to Equation (12) with the chemical reaction terms neglected. The numerical solutions to Equation (12) indicate that T_i should be independent of the initial propellant temperature. By use of this fact it is possible to summarize the results of the numerical calculations. It is found that to an adequate approximation

$$\sqrt{t_i} = \frac{\Gamma\sqrt{\pi}}{2f}\left[\frac{E/R}{1-1.04\ln f/B} - I_o\right] \tag{15}$$

A surface exothermic reaction was considered in the model presented here because it was felt that this was a likely process in the case of a composite propellant. Since any bulk reactions must occur very near to the surface, the assumption of a surface reaction is a good approximation. It should be mentioned that the calculations by Hicks [10] in which he considered a bulk exothermic reaction are in qualitative agreement with the results presented here. The only quantitative difference is that the activation energies calculated from a $\log\sqrt{t_i}$ versus log f plot from Hicks' results are approximately twice the values calculated from Equation 13.

Some work has been done in an attempt to reconcile the low flux ignition results from the radiation furnace, which are adequately described by the simple ignition theory, to the high flux ignition results obtained from the arc image furnace which are not even qualitatively described by a simple thermal theory. The arc image furnace data [15] indicate a large effect of pressure on the ignition times and a very significant increase in the calculated surface temperature at ignition at high surface fluxes. Such behavior is not predicted by the thermal theory. If the radiant energy in the arc image furnace penetrated to a significant depth below the surface, the observed increase in T_i of high fluxes could be explained

In order to account for such a possibility, Equation (12) was modified to allow for transparency of the propellant. In dimensionless form the mathematical relationship describing this model is that

$$\frac{\partial U}{\partial \tau} = \frac{\partial^2 U}{\partial Z^2} + \frac{E}{T_r}e^{-\frac{Z}{T_r}} \tag{16}$$

with the boundary condition at Z = 0 that

$$-\frac{\partial U}{\partial Z} = B_2 \, e^{-\frac{1}{U}},$$

and as $Z \longrightarrow \infty$

$$U = Y$$

The initial condition is that $\tau = 0$

$$U(Z) = Y.$$

The dimensionless parameters are defined as

$$F = f/B, \; U = \frac{R}{E_b} T, \; Z = \frac{R}{E_b} \frac{B}{k} z,$$

$$\tau = \left(\frac{RB}{E_b \Gamma}\right)^2 t \quad \text{and} \quad T_r = \frac{RB}{E_b k} \frac{1}{\lambda} \quad \text{where}$$

$\Gamma = \sqrt{k\rho c}$ and λ is the opacity of the solid.

Numerical solutions were obtained to Equation (16), and Figure 6 shows typical results. A significant increase in T_i is noted as a result of the solid transparency. However, if the effect of pressure is interpreted as the effect of changes in parameter B_2, it is seen that the predicted pressure effect would not be very great.

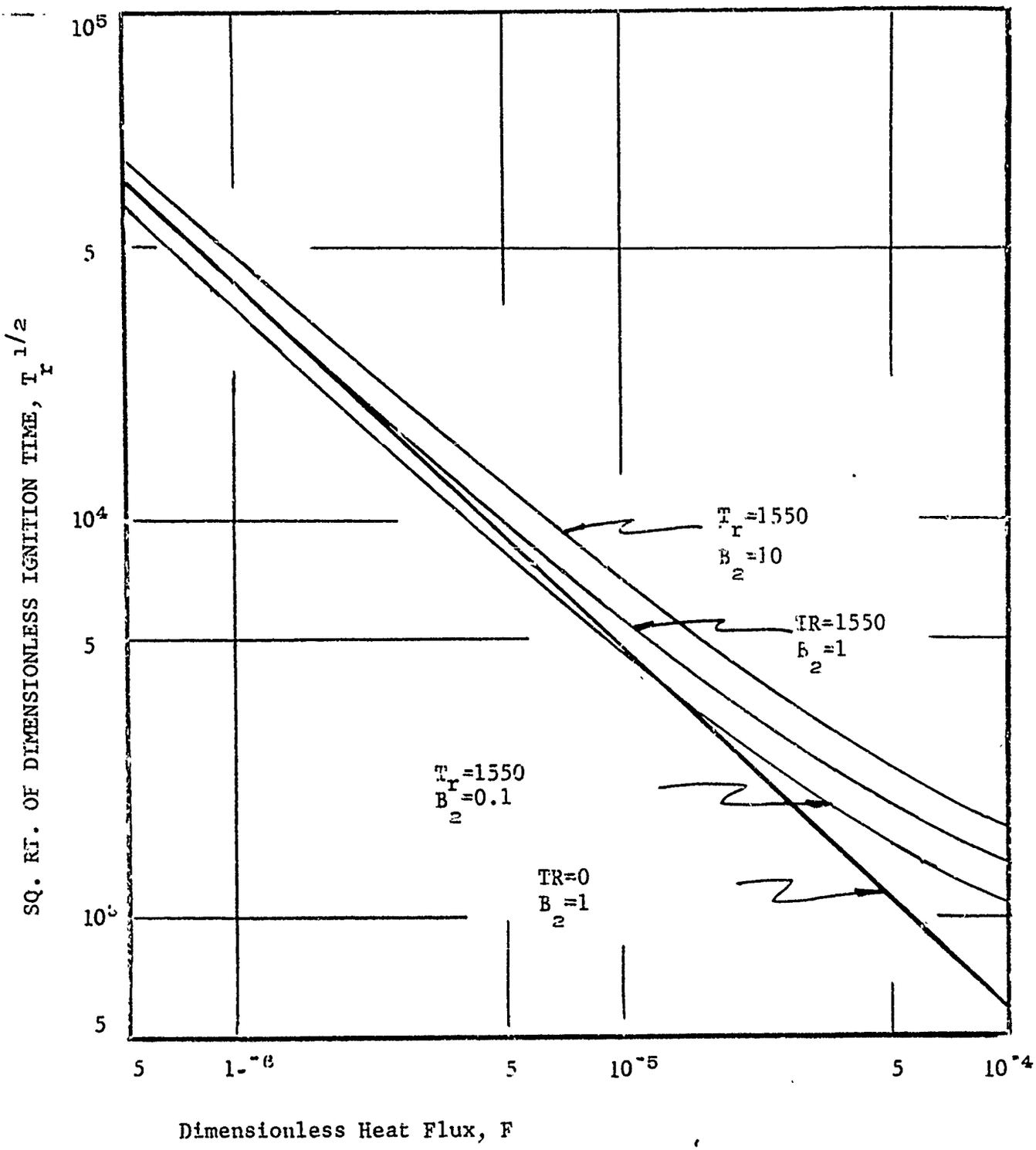

Fig. 6. The Effect of Solid Transparency on Calculated Ignition Times. T_r the dimensionless solid transparency and B_2, assumed proportional to pressure, are defined in Equation (16). The initial dimensionless temperature, Y, is 0.0250.

IV. RADIATION FURNACE TESTS

The analysis of the ignition data obtained in the thermal radiation furnaces appears to be quite straightforward, and a great deal of work has been done in an effort to exploit the capabilities of the apparatus and to gain an understanding of the ignition process. In these furnaces, thermal radiation fluxes ranging from 2-13 cal/(sec)(cm)^2 were employed, and ignition times from .25 to 10 seconds were observed. Under these conditions, the composite propellant can be treated as homogeneous material with respect to its thermal properties, the partial translucence of the propellant constituents to thermal radiation may be neglected or eliminated and the external surface fluxes will always be less than the steady state energy feedback of the burning propellant. Also, because of the relatively long time intervals involved, the propellant ignition time can be accurately taken to be the time of appearance of first flame; and, hopefully, if a chain of reactions occurs, the rate limiting reaction may be easily identified. Direct extrapolation of ignition data obtained under these conditions to the conditions that exist in a rocket engine is not satisfactory, but, once ignition under low flux conditions is understood, a firm base for more complicated theoretical extrapolation is at hand.

Table II summarizes the important thermal and chemical properties of the propellants tested during the course of this work. The FC and GC propellants were simply the F and G propellants with a thin coating of carbon black on the surface exposed to radiation. The FM propellant was similar to the F propellant except 2 per cent carbon black replaced an equal quantity of polymer in the formulation.

In previously reported data [8, 9], the observed ignition times were correlated in terms of the radiation flux inside the black body furnace interior. If the actual surface flux to the propellant is to be calculated, several factors must be evaluated. Since the absorptivity to thermal radiation of the propellant surface is not unity, a correction must be made for the fraction of the incident flux which is reflected from the surface. Measurements on propellants similar to those used in this work indicate that these composite propellants' surfaces can be treated as gray surfaces with an absorptivity from 0.90 to 0.93 [11]. Attempts to determine the absorptivity of the actual propellants used by means of attenuated total reflectance measurements have been unsuccessful mainly as the result of the in-

adequacy of available instrumentation. However, a comparison of the ignition times of carbon black coated surfaces to ignition times of coated surfaces of the same propellant indicated that the absorptivity is very close to 0.9, and an absorptivity value of about .9 was found for the A propellant by an indirect method discussed in a previous report [8] When calculating the surface heat fluxes to the propellant, it was assumed that the surface absorptivity of all fresh-cut surfaces was 0.9. In the carbon black coated surfaces an absorptivity of 1.0 was assumed.

In addition to the energy reflected from the propellant surface, some energy is radiated from the surface. Also, some energy is transferred to the surface by free convection from the high temperature gases in the furnace. Although the effects of radiation from the surface and free convection to the surface tend to be compensating, both of these effects were included as corrections to the furnace radiation flux when calculating the propellant surface heat flux. These surface fluxes were determined from calculated linear surface temperatures at ignition obtained by a numerical technique in which steady state heat transfer coefficients [12] were calculated at the end of each time increment. The calculated surface flux was taken to be the constant flux that would produce the numerically calculated surface temperature at the ignition time. Normally the calculated flux was only 1-2 per cent greater than 0.9 of the radiation flux in the furnace.

By use of this calculation technique, the data previously reported [8] on the effect of pressure on ignition has been corrected for the effect of free convection heat transfer. Figure 7 indicates that in the low flux range the ignition of the A propellant, a typical AP propellant, is a function of the surface heat flux but not a function of pressure.

Experimental Results

Although the ignition character of all ammonium perchlorate oxidized propellants was found to be quite similar when tested in the radiation furnace, it was noted that the ignition times for the F and G propellants were significantly longer than other AP propellants tested. In the case of the F propellant, this effect was the result of partial transparency of the propellant polymer. The same effect was noted for the G propellant; but the fact that this propellant contained no burning rate catalyst accounted for part of the difference. When the surfaces of the F and G propellants were coated with carbon black, the transparency was eliminated and the surface

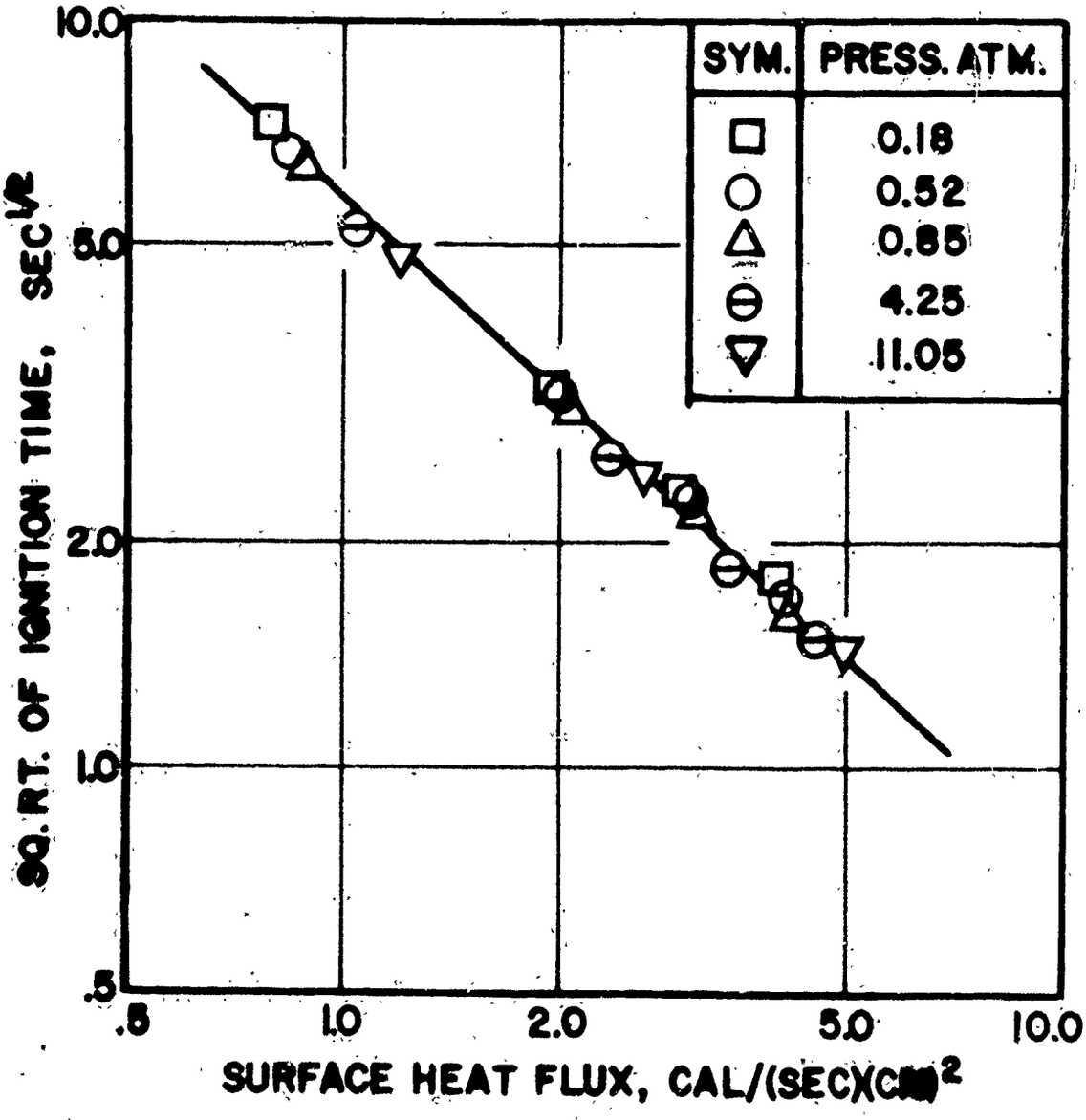

Figure 7. The Effect of Pressure on the Ignition Times of the A-Propellant.

absorptivity was increased from 0.9 to 1.0. Figure 8 summarizes the ignition data for the F, G, FC, GC, and FM propellants. The effect of surface transparency is apparent.

Figure 10 summarizes the ignition data for all catalyzed propellants tested. The FC data is seen to agree with the other results. If opacities of 45 cm^{-1} and 125 cm^{-1} are assumed for the G and F propellants respectively, their ignition times may be calculated from Equation (12) and kinetic parameters determined from the FC and GC data. The dashed lines in Figure 8 represent the calculated ignition times for the transparent F and G propellants. Infra-red absorption spectra for the G polymer indicated that the opacity should be higher at the low fluxes (lower radiation temperature) than at the high fluxes (high radiation temperature). That the transparency is associated with the polymer is shown by the data for the FM propellant presented in Figure 8. Except for the addition of carbon black to darken the polymer, this is the same material as the F propellant. Also, since the assumption of a .9 absorptivity for the FM propellant brings the FM data in line with the FC data, it appears that the surface reflectivity is associated with the ammonium perchlorate.

The difference between the ignition time of the FC and GC propellants shows the effect of the addition of a burning rate catalyst to these propellants. In order to investigate these phenomena further, a series of propellants were prepared in which 0, 0.5, 1.0, 2.0, and 4.0 per cent Harshaw Cu-0202-p copper chromite burning catalyst replaced corresponding amounts of AP, and the ignition times of these materials were determined in the atmospheric radiation furnace. The propellants containing 0 and 2.0 per cent catalyst were respectively the G and F propellants. Table III and Figure 9 summarize the results of these tests. The addition of the burning rate catalyst produced some reduction in the ignition times as more catalyst was added until about the 2 per cent level was reached. The 2 per cent and 4 per cent materials showed essentially identical ignition times. Since the surfaces of these propellants were uncoated, some of the effect seen in Figure 9 was due to the reduction in the transparency of the polymer caused by addition of the catalyst. The coated GC and FC propellants which contained 0 and 2 per cent catalysts respectively showed significantly different ignition times at all surface heat fluxes.

One of the predictions of the thermal ignition theory is that the

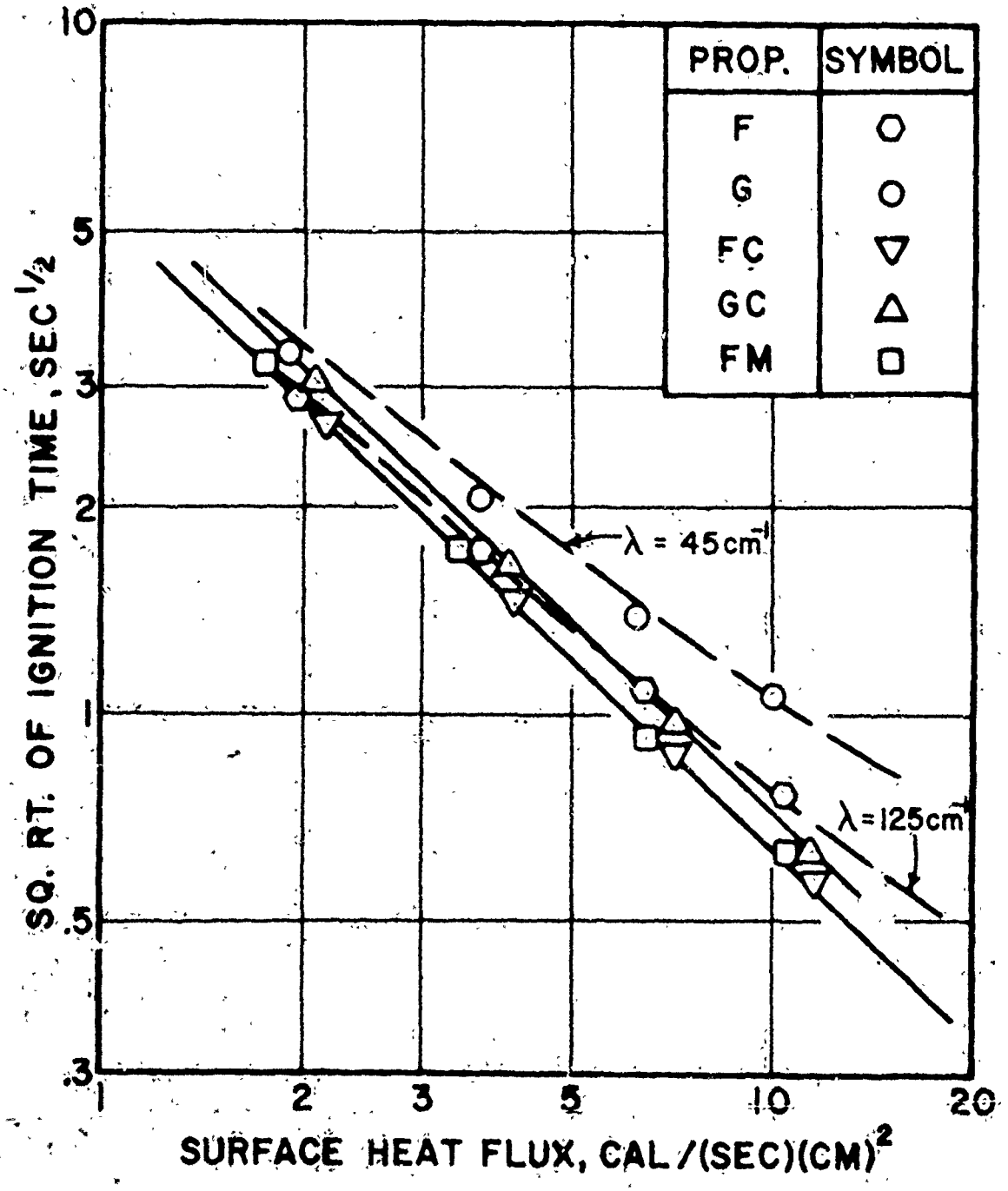

Figure 8. The Effect of Solid Transmissivity on Propellant Ignition Times. The opacity values of 45 cm^{-1} and 125 cm^{-1} are best fit values for the G and F propellants respectively.

FF6 8

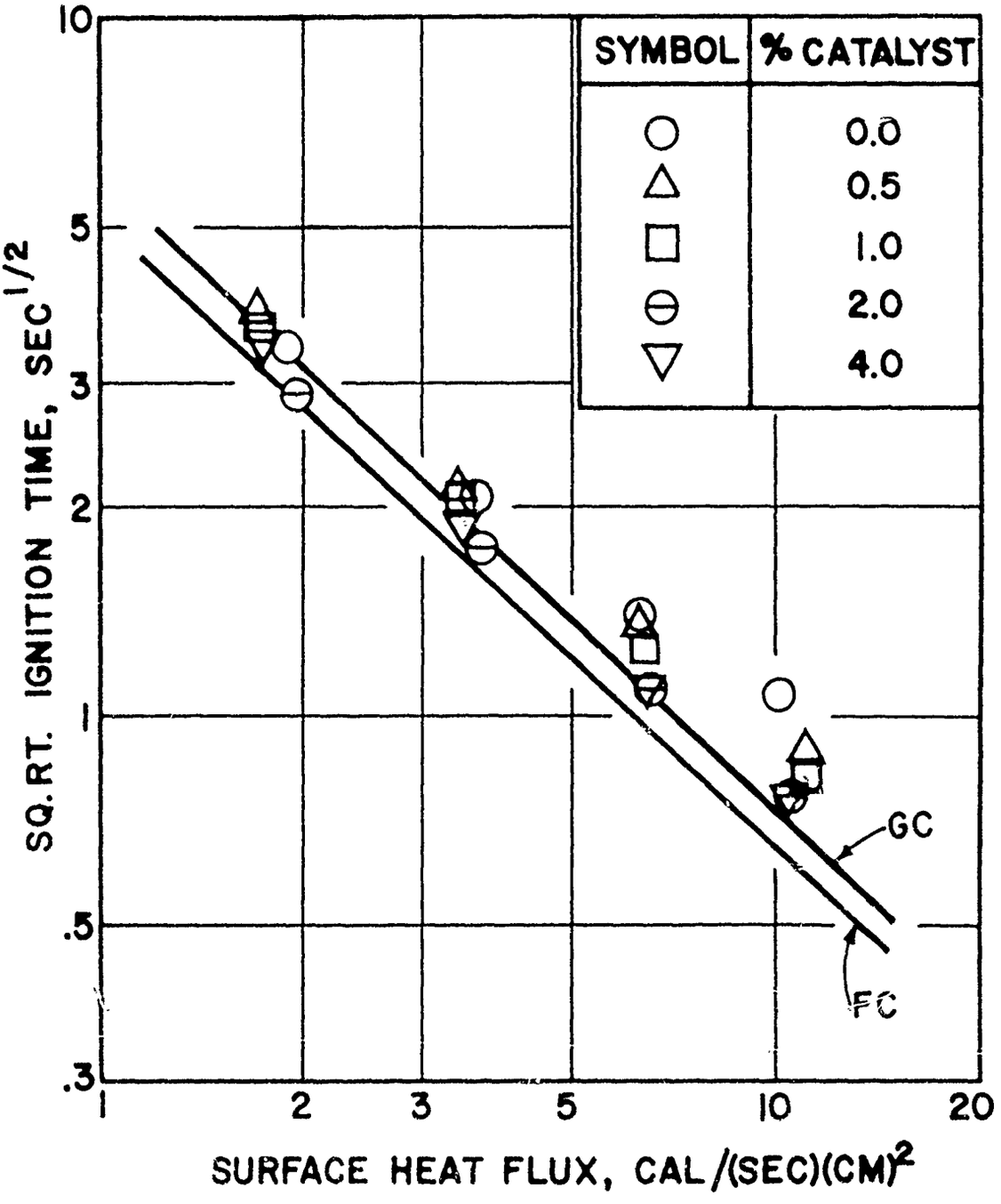

Figure 9. The Effect of the Addition of Copper Chromite Burning Rate Catalyst to the G-Propellant. A comparison of the line for the GC and FC propellants to the data for the 0 and 2 per cent catalyst materials respectively illustrates the effect of the transmissivity of the propellant surface.

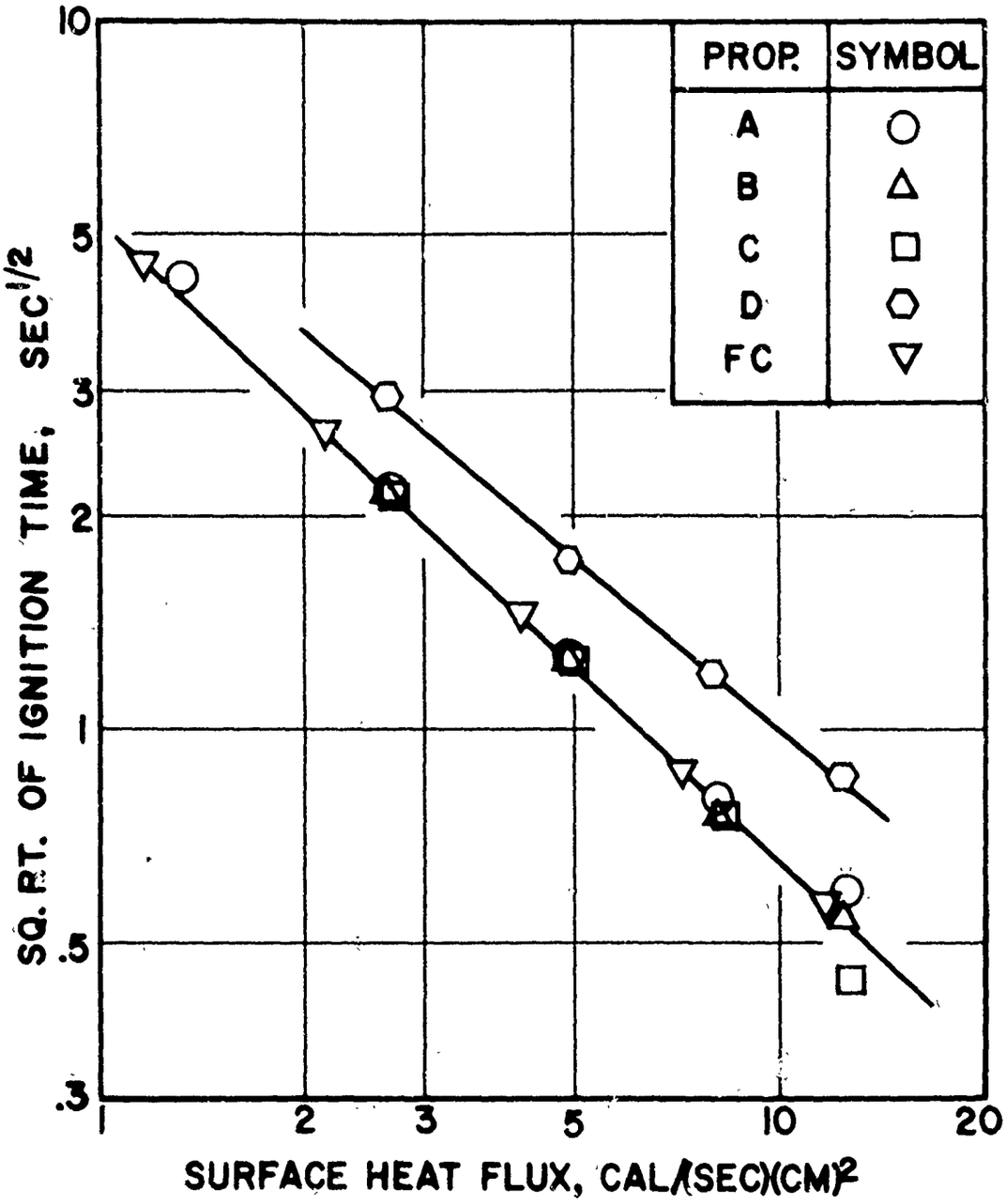

Figure 10. The Effect of Surface Heat Flux on Propellant Ignition Times.

calculated linear surface temperature at ignition, T_i, should be almost independent of the initial propellant temperature [8, 9]. Previously reported data [9] on the ignition of A propellant confirmed this prediction. Some additional tests were made with samples of F and G propellants whose initial temperatures were 50, 25, 0 and -25°C. These samples were subjected to thermal radiation and their ignition times were determined. Tables IV and V summarize these data. Because the tests were made with uncoated surfaces, it was necessary to consider the propellant transparency. At the ignition time

$$T_i - T_o = \frac{2f}{\Gamma} \left(\frac{t_i}{\pi} \right)^{1/2} + \frac{f}{k\lambda} \left\{ e^{N^2} \operatorname{erfc} N^{-1} \right\}$$

where $N^2 = \gamma \frac{kt_i}{c}$ and λ is the propellant opacity. The previously mentioned opacity values of 125 cm^{-1} and 45 cm^{-1} respectively for the F and G propellants were used in the calculation. It is seen in Tables IV and V that the calculated surface temperature at ignition is essentially independent of the initial propellant temperature.

An additional test of the validity of the simple mathematical description of the ignition process was made by considering the ignition characteristics of a square corner section of propellant. The sample holder used in this study is shown in Figure 11. If a two-dimensional (90°) corner is treated as an infinite solid in the direction perpendicular to each face (a semi-infinite corner), it can be shown that, for the case of a constant surface heat flux to each face, the temperature rise at the corner is twice the temperature rise of a semi-infinite body subject to the same surface heat flux. In the case of a square corner with surfaces at $z_1 = 0$ and $z_2 = 0$, the differential equation to be satisfied in the solid is

$$\frac{\partial^2 T}{\partial z_1^2} + \frac{\partial^2 T}{\partial z_2^2} = \left(\frac{k}{\rho c} \right) \frac{\partial T}{\partial t} \qquad (17)$$

with the initial condition of $t = 0$ $T(z_1, z_2) = 0$ for all z_1 and z_2, and

boundary conditions that for $t > 0$ when $z_1, z_2) = 0$ and $z_2 = 0$

$$f = -k \frac{\partial T}{\partial z_1} \text{ and } f = -k \frac{\partial T}{\partial z_2} \text{ and when } z_1 \longrightarrow \infty$$

$$T(z_1, z_2, t) = T(z, t) \text{ and when } z_2 \longrightarrow \infty, T(z_1, z_2, t) = T(z, t)$$

where $T(z, t)$ is the solution to the one dimensional equation

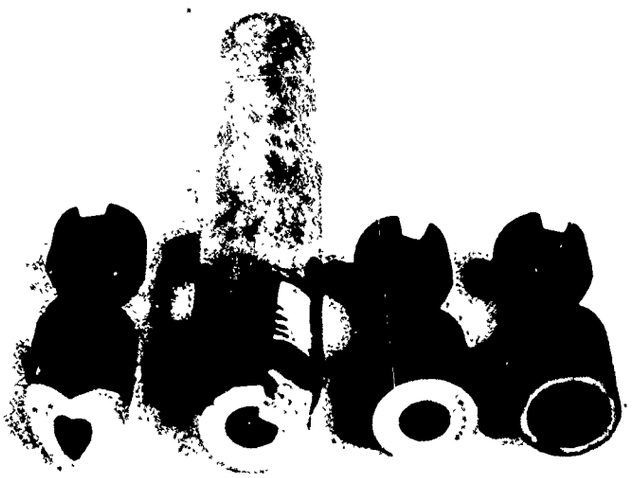

Figure 11. Sample Mountings for the Radiation Furnaces. From right to left the photograph shows: (1) the propellant sample mounted in the sample holder, (2) the mounted sample with edge covered with foil shield, (3) che sample holder projecting from the injection holder as when in the furnace, and (4) the 90-degree corner sample and holder which was used in some tests.

$$\frac{\partial^2 T}{\partial z^2} = \frac{k}{\rho c} \frac{\partial T}{\partial t} \tag{18}$$

for $t = 0$ $T(z) = 0$ when $T > 0$ and $z = 0$

$$f = -k\frac{\partial T}{\partial z} \text{ ; and when } z \longrightarrow \infty \text{ , } T(z,t) = 0$$

It is easily verified by direct substitution that

$$T(z_1, z_2, t) = \left\{ T(z_1, t) + T(z_2, t) \right\}$$

satisfies Equation (17) and the initial and boundary conditions. If $z_1 = z_2 = 0$ or at the corner

$$T(o, o, t) - T_o = 2\left[T(o, t) - T_o \right] = \frac{4f}{\Gamma}\left(\frac{ti}{\pi}\right)^{1/2} \tag{19}$$

A comparison of Equation (19) to Equation (14) shows that the response at a corner is equivalent to the response of a plane surface subjected to twice the energy flux. Thus, if t_i is calculated from Equation (15) for the case of a semi-infinite body, then for the same values of E/R and B, t_i for the semi-infinite corner subjected to the same surface heat flux may be calculated from Equation (15) if the value of f for the corner is taken to be twice f for the semi-infinite body. The ratio of the ignition time for the semi-infinite body to the ignition time of a semi-infinite corner in the radiation furnace at the same temperature should be equal to 3.6. Table VI and Figure 12 represent the results of an experimental check of this hypothesis for the FC and GC propellants and show that for relatively long ignition times the ratio of ignition times is indeed 3.6. The values of E/R and B were determined from the log $\sqrt{t_i}$ versus log F plot for the semi-infinite body. If gas phase reactions at any distance from the surface were important, this predicted relationship between corner and flat surface would not be valid. If ignition occurred at a constant surface temperature, this ratio would be 4.0. The deviation of this ratio from 3.6 in the case of shorter ignition times is the result of the experimental impossibility of cutting a true corner from a propellant slab. Although the samples were carefully cut with a sharp razor blade, microscopic examination showed that the edge of the sample corner had a radius of curvature of about .002 cm. In the case of short-time ignition, the depth of penetration of the energy was not enough greater than the radius of curvature to make the sample respond as a true corner.

Proposed Ignition Mechanism

It has been shown that a relatively simple model which involves consideration of only a single exothermic reaction quite adequately

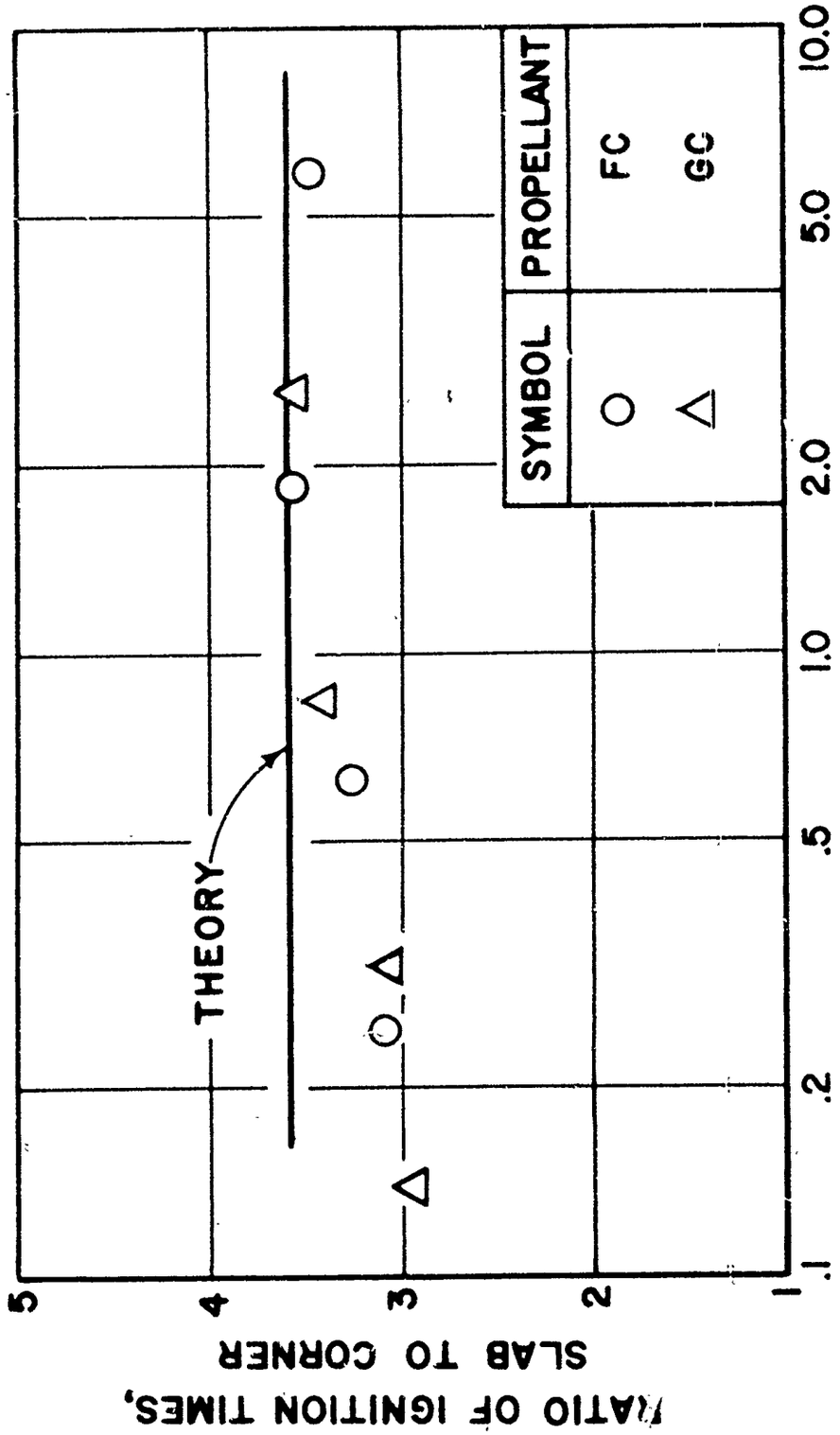

Figure 12. A Comparison of the Ignition Times of Semi-infinite Slabs of Propellant to Semi-infinite 90-degree Corners. The line labeled theory represents the prediction of the simple ignition theory.

describes the ignition process of composite propellants subjected to low level radiant heat fluxes. Some consideration must be given to identifying this reaction in order to justify the simple model. The clue to resolving the gross mechanism of the ignition process of these composite propellants is found in Figure 10. It appears that the ignition times of all catalyzed AP propellants are essentially the same when exposed to the same surface heat flux. Although the thermal properties of all these propellants are fairly similar, a variety of polymers, additives, solids loadings, and burning rate catalysts are represented. The only common component of all the propellants is the ammonium perchlorate. An obvious and convenient hypothesis is that the ignition is controlled by the decomposition of the ammonium perchlorate. Subsequent reaction between the AP decomposition products and solid-fuel binder is also suggested since the data in Figure 10 do not indicate a dependence on polymer or presumably on polymer pyrolysis rates.

In order to test these hypotheses, a series of special propellants containing as non-volatile fuel graphite or carbon black were prepared by pressing mixed powders at 100,000 psi. The carbon black was fired at 1000°C. in an inert atmosphere for two hours prior to use in the propellant. Table VII summarizes the chemical and thermal properties of these materials Ignition times for each propellant were determined in the radiation furnace Table VIII summarizes these data. All propellants showed an easily identifiable flame which was taken as an indication of the ignition and burning. Only the graphite-containing propellant and the ammonium perchlorate which contained two per cent carbon black ceased burning when removed from the furnace.

Because the thermal properties of these materials were not similar, it was necessary to correct the ignition data to a common basis. As indicated previously, Equation (12) was put into dimensionless form before numerical solutions were obtained. A consideration of the dimensionless groups involved in the solutions show that, if the value of B and E/R for a series of propellants is the same, then a plot of log $\sqrt{\frac{t_i}{\tau}}\left(\frac{RB}{E}\right)$ versus log f/B should yield a single line for the series and, for the same surface flux at a given value of $\sqrt{\frac{t}{\tau}}\left(\frac{RB}{E}\right)$, the surface temperatures would be the same. Figure 13 is such a plot for the series of propellants with non-volatile fuel binders; also included are data for the FC propellant. The values of E/R and B were respectively 14,000°K and .46 x 10^{10} cal/(sec)

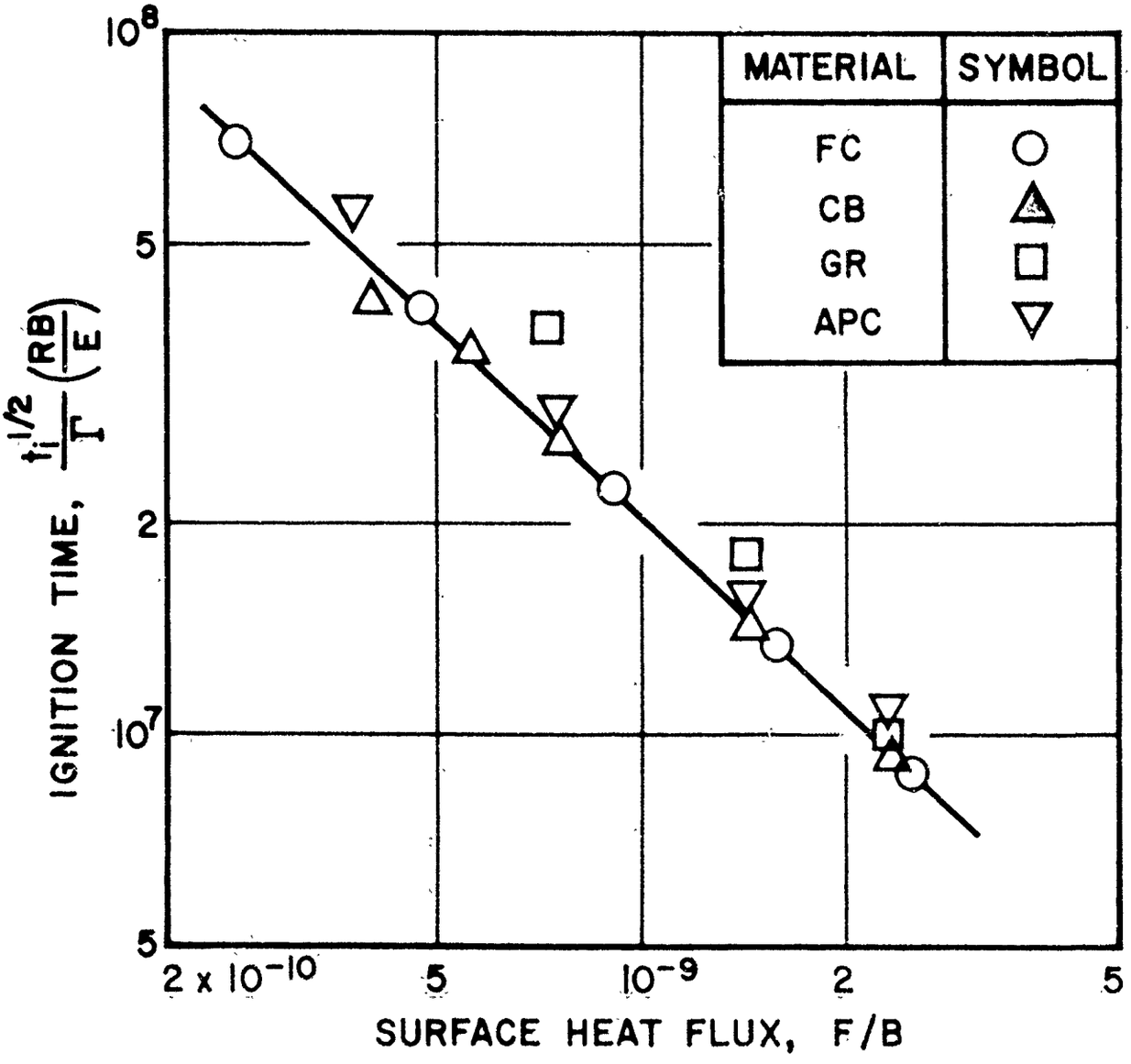

Figure 13. The Ignition Characteristics of Various Materials which Contain Non-volatile Fuel-binders and the FC-Propellant. Data points falling on the line indicate ignition at the same temperature as the FC propellant.

(sq cm). These values were determined from previous ignition data on the FC propellant. With the exception of two points which represent long period ignition of the graphite propellant, a single line results for the FC, CB, and GR materials. APC, which was basically only AP, ignited at a surface temperature a little higher than the other materials. If APC contained somewhat more than 2 per cent carbon black, the ignition times would probably have been identical to the other materials. The conclusion that the ignition proceeds by AP decomposition followed by an exothermic reaction between AP decomposition products and solid-fuel binder seems inescapable. This mechanism is compatible with the simple mathematical model previously proposed. The activation energy of 28 Kcal/g mole calculated from the ignition data is comparable to the activation energy for the anticipated AP decomposition reaction [13], however, considering some of the approximations involved, this agreement may be fortuitous. Since the steady state combustion of carbon black fueled ammonium perchlorate propellants is similar in many respects to the combustion of polymer fueled propellants [14], it appears that a hetrogeneous reaction between AP decomposition products and the solid fuel binder may be important in steady state combustion.

Summary

The ignition of composite rocket propellants subjected to surface heat fluxes in the range from 2-13 cal/(sec)$(cm)^2$ can be described by a very simple mathematical model which considers only a single exothermic propellant reaction. Under these conditions, pressure has little effect on the ignition process. The effect of initial uniform propellant temperature on the ignition time may be treated by making use of the fact that the linear surface temperature at ignition, T_i, is almost independent of the initial temperature. The ignition mechanism, which is consistent with this model, is that the ammonium perchlorate decomposition is the first step in the process, the ammonium perchlorate decomposition products react with solid-fuel binder, and the energy released by the decomposition products and fuel binder quickly brings the propellant to steady state burning conditions.

In the case of ignition of solid propellants subjected to high surface heat fluxes, the situation appears to be more complicated.

Although the high pressure, high-convective heat flux data [3] are reasonably consistent with the results of the low flux ignition tests, most data obtained by use of the high radiant fluxes of the arc image furnace [15] show significant differences, particularly with respect to the effect of pressure. Thus the simple model for low flux ignition probably represents a special case of the general ignition process.

V. IGNITION OF PROPELLANTS UNDER HIGH CONVECTIVE HEAT FLUXES

Several propellant compositions were studied for ignition characteristics under high convective heat fluxes in a shock tube. Heat fluxes in the range of 10 to 120 cal/cm^2 sec were achieved by flowing hot, shock-processed nitrogen over a wall-mounted propellant sample in a test section at the end of the shock tube. This test section (Figure 14) had a rectangular cross-section 0.500 inches by 0.250 inches. The hot gases enter the section through the rounded opening, and a flow control orifice is mounted at the opposite end of the channel The test section has a window directly opposite the sample position, through which ignition of the propellant sample can be observed with a photocell. Heat fluxes at the propellant surface were varied by use of different flow control orifices downstream of the test section and by control of gas temperature and pressure. Periods of essentially constant flux condition were achieved for time intervals of 15 msec at high heat fluxes and 30 to 40 msec at low heat fluxes. The composition of propellants tested during this period is given in Table IX.

It was found in a preliminary investigation that the best method to prepare propellant samples for ignition tests was to cast propellant directly into the sample holders. The sample holders were overfilled with propellant, and a fresh, smooth surface was cut flush with the face of the sample holder immediately before a test.

The primary compositional variable studied was oxidizer particle size. Propellant "F" was the standard reference propellant used for comparison. From these studies it was found that for cut propellant surfaces, ignition times were almost identical at the same heat fluxes for Propellants F, O, P, S, and U. This showed that particle size and oxidizer level in the propellant had little or no effect on ignition times. It was observed, however, that propellants with lower oxidizer levels could be extinguished after ignition with high gas velocities over the propellant surface. Propellant G, which did not contain a burning rate catalyst, could not be ignited. Post-run examination of the G propellant surface showed a charring of the binder. In some cases carbon deposits were found on the lip of the sample holder, but no ignition was detected by the photocell.

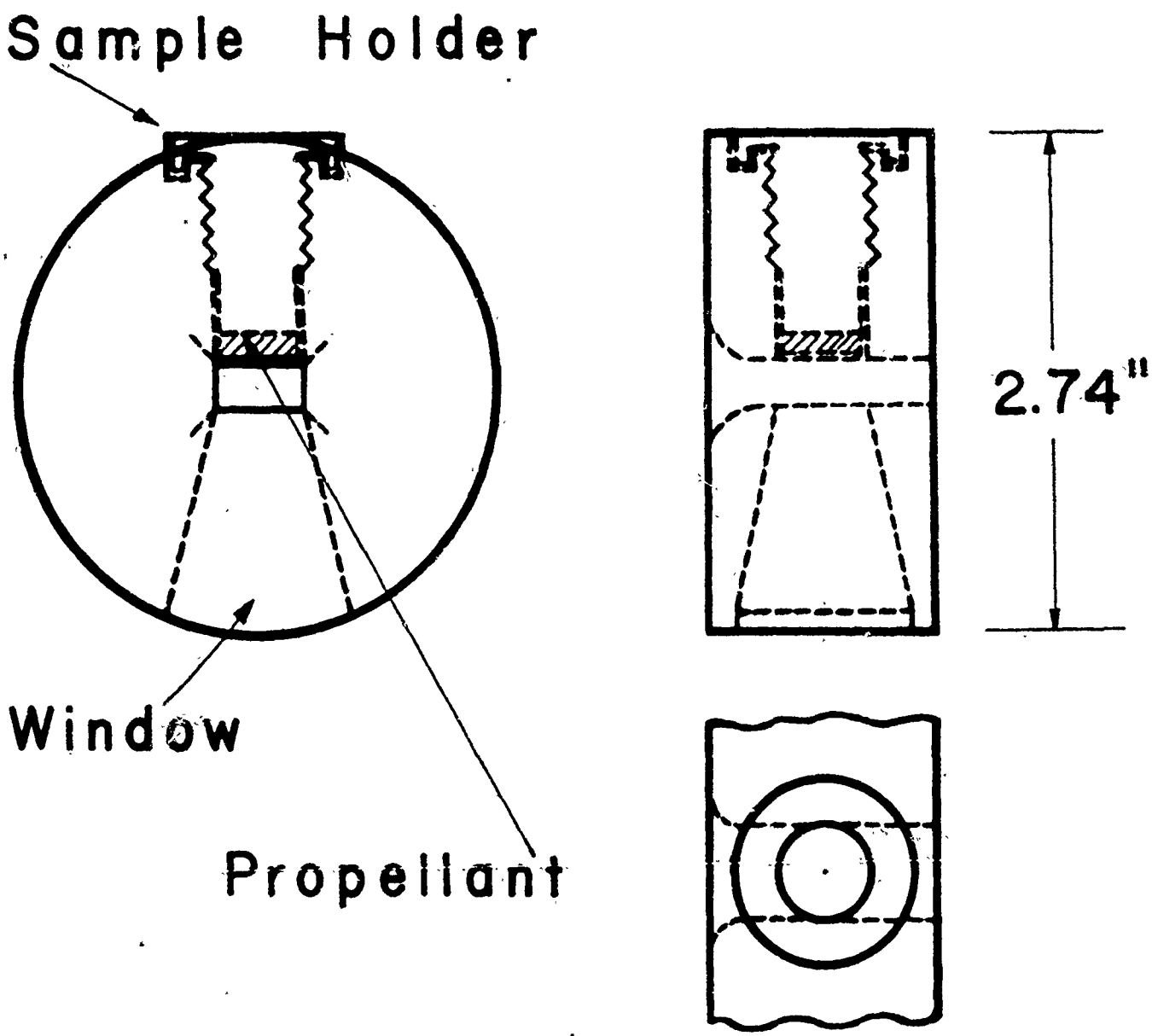

Figure 14.

SHOCK TUBE TEST SECTION

When the surface of the sample was smoothed before curing to produce a thin polymer coat over the oxidizer, it was observed that ignition times were 10 to 15 per cent greater than for a cut surface subjected to the same conditions. Also when this smoothed surface was salted with fine particle size ammonium perchlorate, the ignition times were 10 per cent less than the ignition times of a freshly cut surface. It is possible that these effects are due to increased heat transfer rate as the result of surface roughness. Additional studies will be required to determine the exact nature of this effect.

VI. FUEL-BINDER PYROLYSIS AND OXIDATION

Although some information is available concerning the steady state pyrolysis reactions of propellant fuel binders [16], there is some question concerning the application of these results to the conditions encountered during the ignition process. Most pyrolysis data are obtained by hot plate techniques, and because of assumptions and approximations involved in the analysis of such data, it would be desirable to be able to check the results of such an analysis by an independent method. As mentioned in a previous section of this report propellant ignition data obtained in the radiation furnace strongly indicate that a reaction between solid fuel binder and an oxidizing specie from AP plays an important role in ignition. Also, it is well known that gaseous oxygen can significantly affect propellant ignition, and a possible explanation for this effect would be a heterogeneous reaction between oxygen and the propellant fuel-binder

The above considerations have been the motivation for a study of the propellant fuel binder reactions. The fuel-binder pyrolysis reaction and the reaction between the fuel binder and gaseous oxygen and other oxidizing species are being conducted. Preliminary tests have been made, and while present efforts are intended to improve the experimental techniques, some interesting results have been obtained. A fuel binder composed of polybutadiene acrylic acid and Epon Resin No. 828 in an 85/15 ratio has been studied. Normally, two through four per cent carbon black has been added to reduce the transparency of the solid to thermal radiation.

The Experimental Approach

In this work, films of polymer were coated on the surface of thin film heat flux gages. These gages were constructed of 1 cm diameter x 5 cm long pyrex cylinders; a resistance thermometer was formed on the flat surface of one end by firing an organic platinum paint onto the surface (Hanovia .05 liquid bright platinum). The polymer films covered the resistance thermometers. The surface of the polymer was subjected to heat fluxes ranging from 1 to 4 cal/sec(sq cm) in a sealed thermal radiation furnace.

Two thicknesses of polymer films were used. Because of the relatively long time intervals involved (20 to 50 seconds near the end of the test period), the temperature of the thin polymer films ($\sim$.005 cm thick) was essentially that of the resistance thermometer. As long as the heat flux gage could be treated as a semi-infinite body, the time-temperature information from the gage could be transformed into a time or surface temperature heat flux relationship, and a comparison could be made to the radiation flux in the furnace. The thin polymer film tests were useful in determining the temperatures at which reactions start. For the higher surface flux tests planned, it is doubtful that a polymer film thin enough to be treated in this fashion can be applied to the gage. Thick (.08 to .15 cm) polymer films were employed in some tests. The temperature of the resistance thermometer on the gage lagged significantly behind the polymer surface temperature, and it was necessary to calculate the polymer surface temperature from the properties of the polymer and gage and the gage temperature relationship. Although an analytical solution to the one-dimensional heat conduction equation is known for the case of a surface coating of significant thickness on a semi-infinite body [17], the infinite series representing this solution cannot be conveniently evaluated when thermal conductivity of the surface conductor is less than the conductivity of the semi-infinite body. A numerical solution for this problem was obtained, and analysis of the pyrolysis data was based upon this solution. Both surface and bulk reactions in the polymer can be considered; and if sufficiently accurate data can be obtained, the kinetic parameters of the polymer reactions can be evaluated.

The major experimental problem encountered when applying these techniques has been that the platinum film is apparently altered during a test by reaction products. Significant gage resistance increases have been noted, and the temperature coefficient of resistance of the gages has been greatly altered. Because of this problem, some anomalous results have been obtained, and the results discussed below must be considered as tentative. An apparatus is being assembled which will coat the gage surface with an impervious but very thin layer of SiO_2. This coating is expected to eliminate this problem.

Preliminary Results

Agreement was observed between the calculated and observed gage temperatures during pyrolysis tests on thick polymer films. The main problem was

accurate determination of the polymer film gage thickness. It appears that the first pyrolysis reaction started at 280 to 330°C, and only a small thermal effect of the reaction was noted. The flux levels employed were of the order of 5 cal. per (sq. cm., sec.). The initial pyrolysis reactions may not absorb energy at a rate high enough to be studied by this technique.

The oxygen-polymer reaction was studied in approximately 1, 5, and 10 atmospheres of oxygen. In these tests, the changes in the resistance thermometer properties were quite large. At a total pressure of 1 atmosphere in oxygen or air, it was observed that at a furnace temperature of 800°C, the polymer film charred but did not burn after 50 seconds of exposure while at a furnace temperature of 1100°C, the film was completely consumed. Tests with thin films indicated that a strong reaction started at about 350°C in one atmosphere of oxygen. Tests at higher pressures have so far failed to yield consistent results.

VII. IGNITION BY GASEOUS DIFFUSION FLAME

Among the difficulties associated with the conventional solid rocket ignition systems are that the heat flux distribution throughout the grain is non-uniform, a sharp pressure pulse is developed by the igniter, and the weight of the exhausted ignition and its fixtures must be carried as dead weight by the motor in flight. A suggested technique to overcome these problems is to fill the interior of the grain with oxygen and then to introduce a jet of propane which flows past an ignition source. Hopefully, a large, luminous diffusion flame would develop and produce a smooth pressure rise and a high, uniform interior heat flux. Since the propane could be injected by a pipe through the rocket nozzle, the ignition system would not be carried by the rocket. In order to check this technique, an exploratory research effort was started, and the results of this work are summarized below.

Apparatus and Procedure

Two combustion systems, differing only in size, were used in this experimental work. Figure 15 shows both systems as they appeared in the laboratory ready for firing; and Figure 16 is a schematic diagram applicable to both systems. The essential part of both sets of apparatus were the combustion chamber, the propane injection system, the propane ignition system, and the heat and pressure sensing elements. The apparatus will be discussed under these headings.

Combustion Chamber. The two combustion systems were built and operated to permit a preliminary consideration of scaling problems. The larger apparatus had a combustion chamber with a volume of 200 cubic inches, and the smaller apparatus had a combustion chamber volume of 30 cubic inches. The length to diameter ratio of both chambers was about 6 to 1, and they were constructed so that a geometric similarity existed. Each combustion chamber was made of heavy wall pipe with flanges at each end. Combustion chamber dimensions are tabulated in Table X.

Six holes were drilled and tapped at regular intervals in the side of each chamber to permit installation of the heat flux gages. The surface of the gages was flush with the chamber wall.

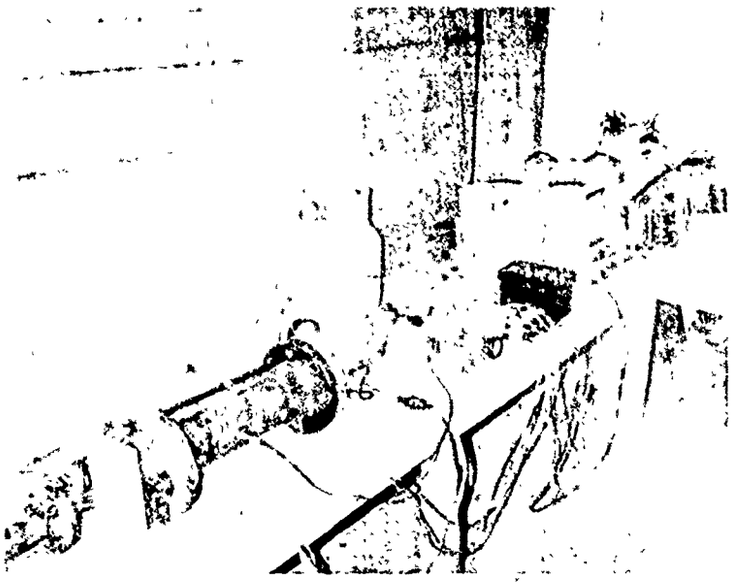

Larger Ignition System

Smaller Ignition System

The pictures above show the experimental apparatus used in investigating propane-oxygen mixtures for solid rocket propellant ignition. On the left, the reservoir chamber appears with the solenoid valve attached and an injection tube running through a shield and into the combustion chamber. The portable triggering switch lays in front of the chambers. The propane tank can be seen and to its right is the variac used to supply current to ignite the mixture. The three instruments that can be seen next on the table are the amplifier used with the pressure gage, the heat flux gage circuitry box, and the automatic timer. The oxygen tank is partially hidden by the two oscilloscopes at the end of the table.

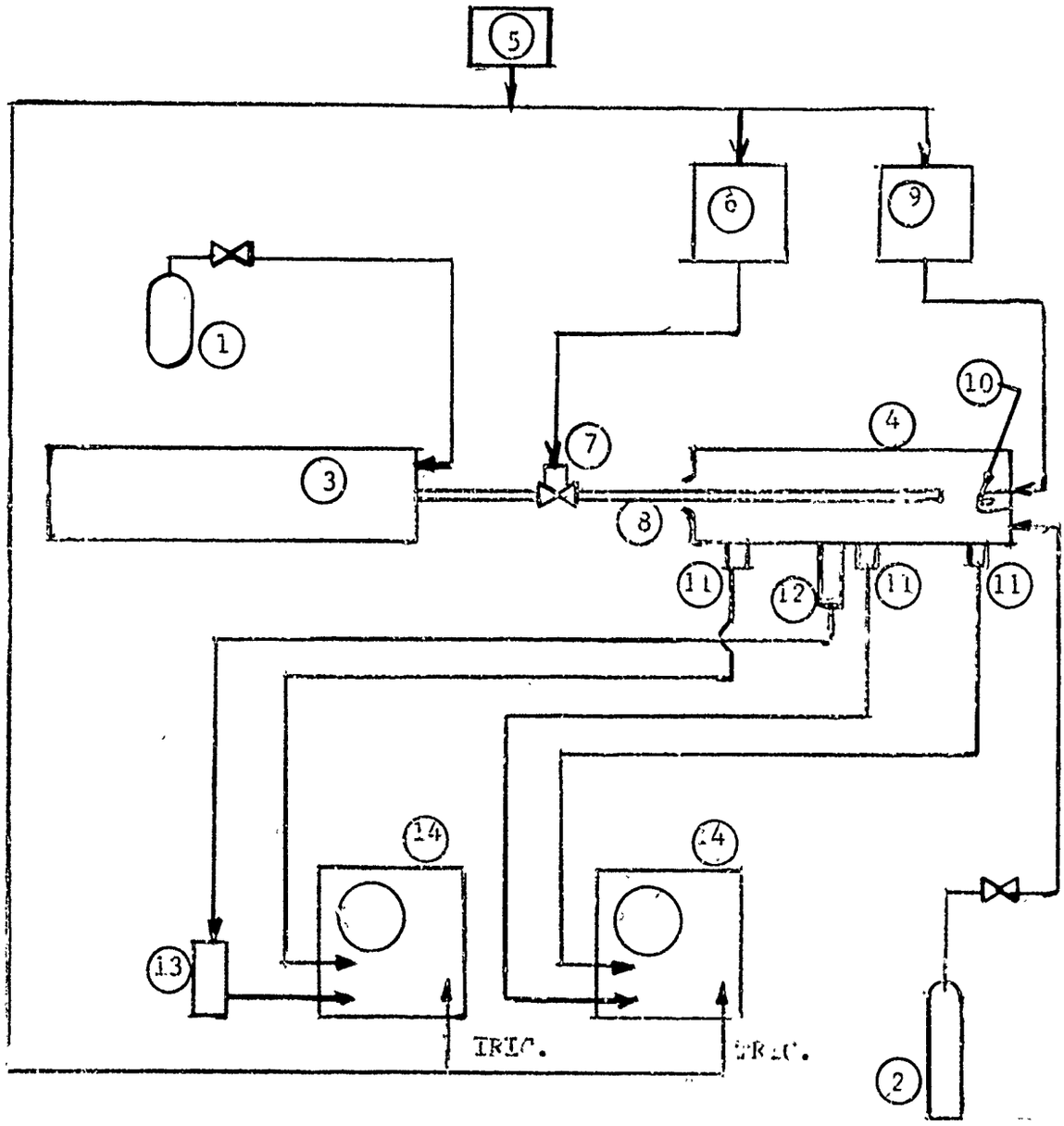

KEY

1. high pressure propane supply
2. high pressure oxygen supply
3. low pressure propane reservoir
4. combustion chamber
5. start switch
6. injection period timer
7. solenoid valve
8. propane injection tube
9. power supply for 10
10. ignition wire
11. heat flux gages, current source not shown
12. pressure transducer
13. amplifier
14. oscilloscopes

Fig. 16. Schematic Diagram of Diffusion Flame Ignition Apparatus.

At one end of the chamber a converging nozzle was attached. The nozzles were sized such that L*, the ratio of the chamber volume to the area of the nozzle, would be about 275 inches. The other end of the chamber was closed by a plate which contained sealed electrical connections to which the ignition wire could be attached. A nichrome wire which was used for ignition of the gas was attached to these connections A vent hole in this plate was connected through valves to a vacuum or to an oxygen supply. The vacuum was supplied by an aspirator, and the oxygen supply was a high pressure cylinder fitted with a pressure regulator.

Propane Injection System. Propane was placed in a low pressure reservoir before it was introduced into the combustion chamber. The reservoir consisted of a pipe with flanges at each end and was similar to the combustion chamber, but lighter in construction The pipe was commercial 1 1/2-inch pipe. The reservoir for the larger system was 81 inches long, and that for the smaller system was 10.8 inches long A single line was connected to one flange. This line was used to bleed the system when it was believed that there might be contaminating gases within the reservoir and also to adjust the pressure within the reservoir The flange on the other end of the reservoir had two pipes extending from it. One line ran to a high pressure propane tank. This line contained a valve adjacent to the reservoir which was used to control the propane flow into the reservoir. The other line was connected to a high pressure solenoid valve. This valve had a 1/4-inch diameter orifice and a response time (closed position to full open) of 4-5 milliseconds. Injection tubes were attached to the other side of the solenoid valve. The injection tubes passed first through a 1/2-inch plywood shield, then through the nozzle, on the combustion chamber, and into the chamber to a point near the ignition wire. Two 14 1/2-inch-long stainless steel injection tubes were used in this experimental work. Their inside diameters were .27 inches and .14 inches.

The solenoid valve was opened and closed by a timer which supplied an electrical pulse to the solenoid of predetermined width with an accuracy of .2% of the pulse time. The timer was controlled by a push button connected to a long electrical cord to permit remote operation. This single push button also triggered the ignition system and the oscilloscopes which were connected to the sensors on the combustion chamber.

Propane Ignition System. Propane flowing into the chamber was ignited by a piece of 22-gage nichrome wire which extended about one inch into the chamber from the head end. When the system was triggered, a pulse of electricity passed through the wire causing it to glow. A similar wire was attached to the variable transformer power supply in series with the wire in the chamber. The transformer voltage was adjusted so that after maintaining the circuit for several milliseconds the external wire melted. This procedure insured that the wire within the chamber, which was cooled by the propane jet, was near its melting temperature.

Heat Flux Measurement. The heat flux to the walls of the combustion chamber was measured with thin-film heat flux gages similar to those used by Vidal [17]. A thin strip of platinum was fired on a pyrex substrate. The platinum strip was used as a resistance thermometer, and a measurement of the surface temperature of the pyrex was obtained. The surface temperature was measured as a function of time, and the heat flux to the wall of the chamber was calculated. The pyrex core was mounted in a steel base with an O-ring seal (Figure 17). The wide part of the core fitted very tightly in the steel base, and contact between the four platinum strips and the steel base was avoided by placing the strips in small grooves in the pyrex. Near the small end of the gage, the fit was somewhat looser to prevent electrical contact with the steel. This type of gage was easily constructed and is easily repaired when the platinum film becomes damaged.

Generally, three heat flux gages were operated simultaneously when obtaining data, and a single current source was used for all three gages. The signals from these gages were recorded on two Model 502 Tektronix Oscilloscopes equipped with Polaroid cameras. A pressure signal was also displayed on one oscilloscope. With these oscilloscopes, the heat flux gage outputs required no external amplification; however, triggering of the oscilloscopes was a problem. The initial temperature (and pressure) rise was so rapid that internal triggering was not satisfactory. The oscilloscopes were triggered at the time the propane solenoid was opened. Because of a non-reproducible delay in the ignition of the gas which occasionally exceeded the oscilloscope sweep time, satisfactory data were not obtained from many tests.

Pressure Measurement. Pressure measurements were made with a Kistler Type 401 Pressure Transducer. The transducer output was amplified by a

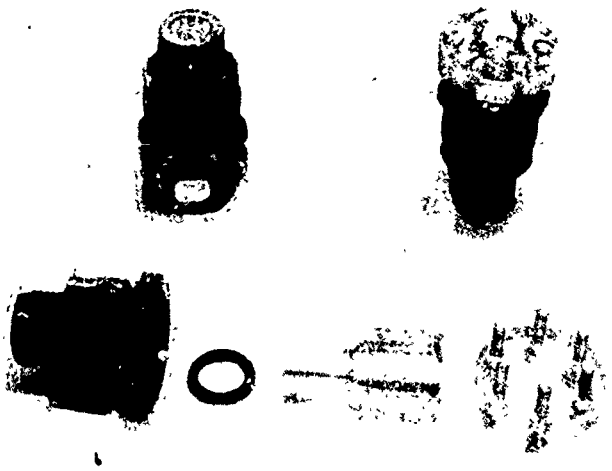

Figure 17.

Heat flux gages for measuring the heat flux to the combustion chamber wall.

Kistler No. 565 Charge Amplifier and was displayed on the oscilloscope screen.

Results

Tests were made by systematically varying propane-oxygen combustion conditions in order that several parameters might be analyzed. The two combustion chambers and two injection tubes have already been discussed. The combustion chambers had volumes of 1.98 cubic inches and 30 cubic inches, and the injection tubes were .27 inches and .14 inches in diameter. Three total propane injection times of .5, .3, and .1 seconds were used; and runs were made with initial propane reservoir pressures of 2.5, 5.0, 7.5, and 10.0 psig.

Figure 18 shows typical results of two ignition tests made under identical conditions. It is evident in these pictures that exact reproducibility of the data was not obtained, and this was generally the case. Erratic temperature fluctuations such as are shown in Figure 18 were apparently caused by the random eddy motion of the gases in the chamber. Eddies of burning propane and oxygen passing over the gage would certainly increase the gage temperature, while eddies consisting of the non-reactive gases which passed near the gage surface might shield the gage from more distant radiation. Because of this randomness it was necessary to make several ignition tests under each set of experimental conditions. At least four, sometimes seven or eight successful firings were made under each set of test conditions.

Although the gaseous ignition occurred up to 100 msec after opening the propane solenoid valve once gaseous ignition started, the pressure in the chamber and the surface temperature of heat flux gages rose quickly to a maximum value. Usually 2-5 msec were required to reach these maximum values, and these values were then maintained for a somewhat longer period. Tables XI and XII summarize the results of a preliminary but systematic study of the process variables. A practical physical meaning can be attached to these results. If the maximum surface temperature was greater than 200°C, ignition of a composite propellant such as A or F propellant would have occurred at that position in the chamber under the experimental conditions. The data in Tables XI and XII indicate that the highest values of surface temperature

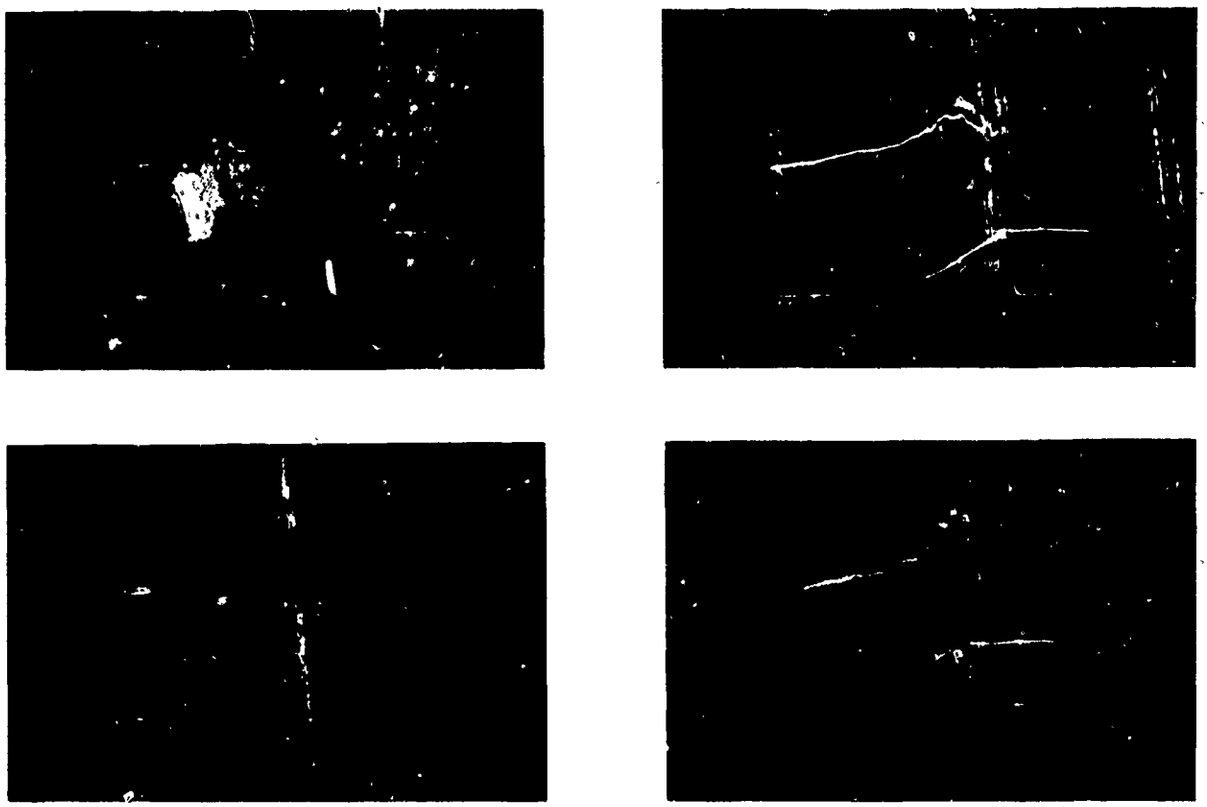

Figure 18. Oscilloscope record of temperatures and pressures for two similar tests. The test conditions (number 1111) were: reservoir pressure, 5 psig; injection time, .5 seconds; 30 cubic inch combustion chamber; and a .14 inch inside diameter injection tube. Time increases from right to left. The upper curve in both right hand pictures is the heat flux gage surface temperature taken near the head end of the chamber (25.6°C/division) and the lower one shows the pressure near the midpoint in the chamber (20 psi/division). The single trace in both of the left hand pictures shows the temperature near the midpoint of the chamber (25.2°C/division). The time scale on the left is 2.5 milliseconds/division, and that on the right is 5 milliseconds/division.

and pressure. and time were obtained under conditions of maximum rate of propane injection. Injection periods greater than 0.1 second did not appear to influence the results. The highest temperatures were normally recorded by the gage placed in the center of the chamber.

The surface temperature of the gages usually rose rapidly, peaked, fell slightly, and then started to rise again, all within a few milliseconds of ignition, and this type of behavior seemed to be more than a random occurrence in the test results. This type of behavior can be seen in most of the temperature traces in Figure 18. These minute details of the rising and falling temperatures were lost in the averaging of the data. The explanation of the peculiar behavior, provided by high-speed motion pictures that showed periodic oscillations in the flame intensity, is that strong acoustic waves in the fundamental axial mode were excited.

Normal gaseous ignition appeared not to have occurred as the propane first passed the ignition wire, but rather the propane was ignited after striking the end of the chamber and returning to the wire a second time at a lower velocity. The high-speed motion pictures confirmed this hypothesis.

In a small fraction of the runs made with the small combustion chamber, a very different type of ignition occurred, which was characterized by prolonged gaseous burning times and lower gage surface temperature rises. Quantitative information about this type of ignition was not obtained because it occurred almost simultaneously with the initiating electrical pulse. This second type of ignition apparently occurred when the propane was ignited with the first pass across the wire. It is interesting that this second type of ignition never occurred in the larger chamber.

Summary

The experimental results show that surface heat fluxes high enough to produce propellant in a few milliseconds can be obtained from the gaseous diffusion flame. Because the fraction of energy transferred by radiation and by convection was not determined, it would be difficult to predict the scaling laws for this ignition system. Sharp pressure rises were noted, and it appears that these resulted from delayed ignition of the propane. A true diffusion flame was probably not obtained with the ignition system employed. The major objective of future work will be to obtain smooth ignition and combustion at the point of entry of the propane.

Table I.

Calculated Flame Spread

for $\psi(\alpha y) = (1 + \alpha y)^{-1/2}$

Time, $\tau = \beta t$	Position, αx	$d(\alpha x)/d\tau$	$d^2(\alpha x)/d\tau^2$
1	0	--	--
1.1	0.126	(1.4)	--
1 25	0.367	1.8	--
1.5	0.880	2.31	1.9
1.75	1.515	2.76	1.8
2	2.261	3.19	1.6
2.5	4.040	3.92	1.3
3	6.156	4.53	1.15
4	11.22	5.56	0.91
5	17.21	6.40	0.76
6	23.97	7.10	0.65
8	39.35	8.24	0.50
10	56.77	9.14	0.41
12.5	80.81	10.05	0.33
15	106.90	10.80	0.27
17.5	134.72	11.44	0.24
20	164.01	11.99	0.21

TABLE NO. II

SUMMARY OF PROPELLANT CHEMICAL AND THERMAL[1] PROPERTIES

Propellant	A	B	C	D	F[2]	G
Fuel Binder	Polysulfide	Polyurathane	BD/MVP Rubber	BD/MVP Rubber	PBAA	PBAA
Oxidizer Crystal	AP	AP	AP	NH_4NO_3	AP	AP
Approximate Weight Per Cent:						
Oxidizer Crystal	76	82	86	84	80	82
Aluminum	2	2	0	0	0	0
Catalyst[3]	1	in fuel	2	2	2[3]	0
Fuel Binder	21	16	12	14	18	18
Density gr/cc	1.75	1.70	1.70	1.53	1.63	1.60
Thermal Diffusivity cm^2/sec	.00167	.00139	.00196	.00196	.00170	.00171
Thermal Responsivity $(\Gamma = \sqrt{k\rho c})$ $cal/(sec)^{1/2}(cm)^2(°C)$	.0229	.0202	.0233	.0270	.0212	.0206

[1] These values are at approximately 60° C. For calculation purposes, the surface absorptivity was assumed to be 0.9 for the propellants.

[2] The FC propellant was the same as F except a surface coating of carbon black was used during testing and an absorptivity of 1.0 was assumed.

[3] The F propellant catalyst was Harshaw Chemical Co. Cu-0202-p copper chromite. The other catalysts were various compounds of iron.

TABLE III

The Effect of a Burning Rate Catalyst[1] on the Radiation Furnace Ignition Times on PBAA-AP Propellant Formulations

Propellant	Per cent Catalyst	Furnace Temp. °K	Calculated surface heat flow cal/(sec) (sq cm)	Ignition time, sec.
G	0.0	1110	1.91	11.5
G	0.0	1310	3.64	4.34
G	0.0	1508	6.32	1.97
G	0.0	1705	10.16	1.15
	0.5	1083	1.72	14.5
	0.5	1283	3.38	4.60
	0.5	1508	6.35	1.85
	0.5	1730	10.92	6.80
	1.0	1083	1.74	13.0
	1.0	1283	3.39	4.40
	1.0	1508	6.40	1.58
	1.0	1730	11.00	0.68
F[2]	2.0	1110	1.96	8.40
F	2.0	1310	3.72	3.13
F	2.0	1508	6.45	1.20
F	2.0	1705	10.47	0.59
	4.0	1083	1.75	11.8
	4.0	1283	3.43	3.63
	4.0	1508	6.48	1.21
	4.0	1703	10.34	0.58
FM[3]	2.0	1083	1.76	10.8
FM	2.0	1283	3.46	3.16
FM	2.0	1508	6.55	0.87
FM	2.0	1703	10.53	0.41

[1] The catalyst was Harshaw Chemical copper chromite Cu-0202-p.

[2] The catalyst replaced corresponding quantities of AP.

[3] Two per cent carbon black replaced 2 per cent polymer in this propellant.

TABLE IV

The Effect of Initial G-Propellant Temperature on the Linear Surface Temperature at Ignition (T_i)

Initial temp. °K	Furnace temp., °K	Ignition time, sec.	Surface flux cal/(sec)(sq cm)	Surface temp. measured	Ignition[1] °K average
329	1095	10.61	1.79	605	
301	1097	13.12	1.80	605	
277	1098	14.80	1.81	614	609
243	1098	16.78	1.82	612	
329	1300	4.02	3.51	636	
301	1303	4.45	3.55	632	
277	1304	5.20	3.56	640	633
248	1304	5.48	3.59	626	
329	1520	1.60	6.51	647	
301	1511	2.06	6.32	666	
277	1508	2.40	6.26	675	662
248	1513	2.46	6.38	660	
329	1677	1.00	9.45	670	
248	1695	1.24	9.99	662	668

[1] These temperatures were calculated for an assumed reflectivity of 0.1 and an opacity (λ) of 45 cm^{-1}. These temperatures are probably high since they were calculated for assumed constant (60°C) thermal properties.

TABLE V

The Effect of Initial F-Propellant Temperature on the Linear Surface Temperature at Ignition ($v_{s_i}^L$)[1]

Initial temp. °K	Furnace temp. °K	Ignition time, sec.	Surface flux cal/(sec)(sq cm)	Surface temp., Measured	Ignition[1] °K Average
329	1096	7.85	1.85	589	
301	1097	9.23	1.87	587	
277	1098	11.56	1.86	598	589
248	1098	12.88	1.88	580	
329	1293	2.73	3.54	610	
301	1303	3.24	3.64	619	
277	1302	3.84	3.63	625	616
248	1304	3.99	3.68	609	
329	1523	0.95	6.73	625	
301	1507	1.22	6.46	628	
277	1511	1.36	6.53	626	626
248	1513	1.50	6.58	623	
329	1677	0.53	9.82	634	
248	1695	0.68	10.29	618	626

[1] These temperatures were calculated for an assumed reflectivity of 0.1 and an opacity (λ) of 125 cm^{-1}. These temperatures are probably high since they were calculated for assumed constant (60°C) values of the thermal properties.

TABLE VI

A Comparison of the Ignition Times of Semi-infinite Bodies to Semi-infinite Corners of FC and GC Propellants

Initial Temperature 28±2°C

Propellant	Furnace temp., °K	Ignition time of Semi-infinite surface[1] sec.	Ignition time of Semi-infinite corner[1] sec.
FC	950	20.5 ± .70	5.89 ± .24
FC	1110	6.92 ± .14	1.94 ± .23
FC	1310	2.11 ± .05	.65 ± .04
FC	1508	0.76 ± .037	.25 ± .026
FC	1705	0.32 ± .014	.10 ± .019
GC	1110	9.30 ± .36	2.61 ± .17
GC	1310	2.77 ± .11	.82 ± .093
GC	1508	0.97 ± .035	.32 ± .03
GC	1705	0.42 ± .012	.14 ± .03

[1] These numbers represent the average of 5 runs. Average deviations are indicated.

TABLE NO. VII

SUMMARY OF CHEMICAL AND THERMAL[1] PROPERTIES
OF PRESSED MATERIALS

Material	CB	GR	APC
Fuel	Carbon black[2]	Graphite	Carbon black[2]
Wt. Per Cent:			
Ammonium Perchlorate	82.0	82.0	96.0
Fuel	16.0	16.0	2.0
Copper Chromite Catalyst	2.0	2.0	2.0
Density gr/cc	1.65	1.97	1.89
Thermal Diffusivity cm^2/sec	.0024	.0078	.0021
Thermal Responsivity $(\Gamma = \sqrt{k\rho c})$ $cal/(sec)^{1/2}(cm)^2(°C)$	.021	.046	.025

[1] These values are at approximately 60° C. For calculation purposes the surface absorptivity of these materials was assumed to be 0.9.

[2] The carbon black was commercial Phil Black-E previously fired at 1000° C. for two hours.

TABLE VIII

Summary of Ignition Data for Pressed Propellant-like Materials and for the FC and GC Propellants[1]

Initial Temperatures 28±2°C.

Material	Furnace temp, °K	Ignition time sec.	Calculated surface heat flux, cal/(sec)(sq cm)	Square Root[2] of dimensionless equations	Dimensionless[2] Heat Flux
APC	1083	17.2	1.72	5.66×10^{7}	$.378 \times 10^{-9}$
APC	1283	4.6	3.42	2.94	.752
APC	1508	1.35	6.50	1.59	1.428
APC	1703	0.65	10.46	1.10	2.300
GR	1283	28.4	3.29	3.80	.724
GR	1508	6.54	6.43	1.82	1.411
GR	1703	1.98	10.52	1.00	2.31
CB	1083	7.10	1.82	4.15	0.400
CB	1183	5.15	2.53	3.54	0.555
CB	1283	2.78	3.48	2.60	0.764
CB	1508	0.84	6.56	1.43	1.440
CB	1703	0.35	10.57	0.92	2.32
FC	950	20.5	1.15	7.00	.252
FC	1110	6.92	2.15	4.06	.471
FC	1310	2.11	4.14	2.25	.909
FC	1508	0.76	7.22	1.35	1.581
FC	1705	0.32	11.70	0.88	2.500
GC	1110	9.30	2.08		
GC	1310	2.77	4.07		
GC	1508	0.97	7.14		
GC	1705	0.42	11.62		

[1] These propellants were the F and G propellant with a thin surface coating of carbon black. These were the only materials discussed to have a zero surface reflectivity.

[2] The dimensionless ignition times and heat fluxes were calculated as $\tau i = t_i \frac{\Gamma RB}{E}^2$ and $F = fs/B$. In all cases, E/R was 14000°K and B was 4.6×10^{-9} cal/(sec) (sq cm). Thermal responsivities, Γ, for each material was the measured value at 60°C.

TABLE IX

Composition of Propellants used in the Shock Tube Tests

Propellant Code	PBAA Binder (%)	Catalyst Copper Chromite Cu0202-p (%)	Ammonium Perchlorate (%)	Approximate Particle Size of AP (microns)
F	18.0	2.0	40.0	250
			40.0	15
G	18.0	0.0	41.0	250
			41.0	15
O	18.0	2.0	20.0	250
			60.0	15
P	23.0	2.0	37.5	250
			37.5	15
S	23.0	2.0	75.0	100
U	23.0	2.0	75.0	15

TABLE X

Combustion Chamber Dimensions
(All dimensions are in inches)

	Large Chamber	Small Chamber
Diameter	3.50	1.895
Length	20.8	10.58
Nozzle Diameter	1.00	.36
Distance between gage holes	2.7	1.4
Distance from nozzle end to nearest gage hole	3.6	1.85
Distance from head end to nearest gage hole	3.8	1.78
Distance between ignition posts	1.8	1.2
Approximate distance from end of injection tube to head end of chamber	2.3	1.5
Length of ignition posts	.58	.48

TABLE XI.

Summary of Data from Small Diffusion Flame Ignition Chambers

Runs No.	Injection tube diameter in.	Propane pressure psig	Injection period sec	Direction of pressure pulse msec	Maximum pressure psig	Time at max.temp. msec	Maximum Temperature Rise at[1] Gage 1 °C	Gage 2 °C	Gage 3 °C
1111	0.14	5.0	0.5	26	41	16	135	205	--
1112	0.14	5.0	0.3	24	49	18	140	245	--
1113	0.14	5.0	0.1	23	47	15	165	195	--
1121	0.14	10.0	0.5	22	84	16	225	325	--
1122	0.14	10.0	0.3	22	87	18	190	300	--
1123	0.14	10.0	0.1	23	80	18	175	305	--
1131	0.14	7.5	0.5	24	63	17	225	300	--
1132	0.14	7.5	0.3	23	65	17	175	290	--
1133	0.14	7.5	0.1	24	61	17	195	315	--
1141	0.14	2.5	0.5	12	13	12	70	45	--
1142	0.14	2.5	0.3	20	15	10	55	65	--
1143	0.14	2.5	0.1	23	15	9	60	45	--
1211	0.27	5.0	0.5	30	37	19	155	125	90
1212	0.27	5.0	0.3	24	34	17	175	125	90
1232	0.27	7.5	0.3	38	26	58	160	255	195
1242	0.27	2.5	0.3	15	3	13	25	20	25

[1] Gages 1, 2, and 3 were located 8.8-inches, 6.0-inches, and 3.25-inches respectively from nozzle end of the chamber.

TABLE XII

Summary of Data from Large Diffusion Flame Ignition Chamber

Runs No.	Inj. tube diameter in.	Propane Pressure psig	Injection period Msec	Duration of pressure pulse Msec	Max. pressure psig	Time at max. temp Msec	Maximum Temperature Rise at[1] Gage 1 °C	Gage 2 °C	Gage 3 °C
2111	0.14	5.0	0.5	16	12	15	115	100	60
2112	0.14	5.0	0.3	26	16	20	110	90	25
2113	0.14	5.0	0.1	27	17	21	100	105	30
2121	0.14	10.0	0.5	27	60	55	185	400	165
2122	0.14	10.0	0.3	27	54	50	250	450	160
2131	0.14	7.5	0.5	27	38	40	205	320	105
2141	0.14	2.5	0.5	12	3	4	15	75	75
2211	0.27	5.0	0.5	27	12	11	40	40	15
2221	0.27	10.0	0.5	27	30	35	235	320	65
2231	0.27	7.5	0.5	24	24	21	140	130	45
2241	0.27	2.5	0.5	14	4	6	30	10	75

[1] Gages 1, 2, and 3 were located 17.0, 11.5, and 6.3 inches respectively from the nozzle end of the chamber.

NOMENCLATURE

B	constant in Equation (1).
B_2	diminsionless constant in Equation (16).
c	solid heat capacity, cal/gm-°C.
f	surface heat flux, cal/cm^2-sec.
f_1	surface heat flux, cal/cm^2-sec.
f_2	surface heat flux, cal/cm^2-sec.
f_o	heat flux at edge of burning zone, cal/cm^2-sec.
F	dimensionless surface heat flux, see Equation (16).
E_b	Ahrennius activation energy of a surface reaction, cal(g mole)
k	thermal conductivity, cal/cm-sec-°C.
n	exponent for one family of heat flux decay functions, $(\alpha\dot{y}) = (1 + \alpha v)^{-n}$.
p	pressure during the rarefaction "plateau" or pressure, atm.
r	propellant burning rate, cm/sec.
s	intermediate time variable, sec or msec.
t_i	ignition time at position x, with time zero set at the start of gas flow, or ignition times sec or msec.
t_o	ignition time at x = 0.
T	surface temperature rise above T_o, °C.
T_i	calculated value of T at ignition.
T_r	dimensionless propellant transmissivity, see Equation (16).
u	gas velocity during the rarefaction "plateau", m/sec.
U	dimensionless temperature, see Equation (16).
x	distance from the position of the flame front at time zero, measured downstream in the direction of gas flow, cm.
y	auxiliary position variable defined, for a given x, as the distance from the position of the flame front at time s to position x, cm.
Y	dimensionless initial temperature, see Equation (16).
z	normal distance measured into propellant from surface, cm.
Z	dimensionless normal distance measured into propellant from surface, see Equation (16).

NOMENCLATURE (continued)

Greek

α	distance parameter whose purpose is to form the dimensionless distance variables αx and αy, cm^{-1}.
β	time parameter equal to $\frac{4f_o^2}{\Gamma T_i^2}$, used to form the dimensionless time variable τ, sec^{-1}.
Γ	thermal responsivity = $\sqrt{k\rho c}$.
θ	time at which temperature T exists at x, sec or msec.
λ	propellant opacity, cm^{-1}.
ρ	solid density, gm/cc.
τ	dimensionless time variable = βt.
τ'	dimensionless time variable, see Equation (16).
Φ	function defined by Equation (6), determined by Equation (5).
Ψ	heat flux decay function defined by $f = f_o \psi(\alpha y)$.

LIST OF REFERENCES

1. Altman, D., and A. F. Grant, Thermal Theory of Solid-Propellant Ignition by Hot Wires, Fourth Symposium on Combustion, 158, The Williams and Wilkins Co., Baltimore (1953).

2. Baer, A. D., Ignition of Composite Rocket Propellants, Ph.D. Thesis, University of Utah (1959).

3. Baer, A. D., N. W. Ryan, and D. L. Salt, Propellant Ignition by High Convective Heat Flux Fluxes, Solid Propellant Rocket Research, 653, Academic Press, New York (1960).

4. Carslaw, H. S., and J. C. Jaeger, Conduction of Heat in Solids, 2nd edition, Oxford University Press, Oxford (1959).

5. Keller, J. A., Personal Communication (1963).

6. McCune, C. C., Solid Propellant Ignition Studies in a Shock Tube, Ph.D. Thesis, University of Utah (1961).

7. Mitchell, R. C., Flame Spread on Solid Propellant, Ph.D. Thesis, University of Utah (1963).

8. Ryan, N. W., A. D. Baer, J. A. Keller, and R. C. Mitchell, Final Technical Report on Ignition and Combustion of Solid Propellants, AFOSR 2225 (1961).

9. Ryan, N. W., A. D. Baer, J. A. Keller, and R. C. Mitchell, Technical Report on Ignition and Combustion of Solid Propellants, AFOSR Grant 62-99 (1962).

10. Hicks, B. L., Theory of Ignition Considered as a Thermal Reaction, J. Chem. Phys., 22, 414 (1953).

11. Fishman, N., Personal Communication (1963).

12. McAdams, W. H., Heat Transmission, 3rd edition, McGraw-Hill Book Co. New York, 173 (1954).

13. Jacobs, P. W. M., and A. R. TARIQ Kureisky, The Effects of Additives on the Thermal Decomposition of Ammonium Perchlorate, Eight Symposium on Combustion, The Williams and Wilkins Co., Baltimore, 672 (1962).

14. Adams, G. K., B. H. Newman, and A. B. Robins, The Combustion of Propellants Based Upon Ammonium Perchlorate, Eight Symposium on Combustion, The Williams and Wilkins Co., Baltimore, 699 (1962).

15. Beyer, R. B., and N. Fishman, Solid Propellant Ignition Studies with High Flux Radiant Energy as a Thermal Source, Solid Propellant Rocket Research, Academic Press, 673 (1960).

16. Chaiken, R. F., W. H. Andersen, M. K. Barsh, G. Moe, and R. D. Schultz, Kinetics of the Surface Degradation of Polymethylmethacrylate, J. Chem. Phys., 132, 144 (1960).

17. Vidal, R. J., Model Instrumentation Techniques for Heat Transfer and Force Measurement in a Hypersonic Shock Tunnel, Cornell Aeronautical Laboratory Report No. AD-917-A-1, WADC-TN-56-315, ASTIA No. AD-97238 (1956).